NTNU – Trondheim
Norwegian University of
Science and Technology

Python Framework for Design and Simulation of Integer-N ADPLLs

Cole Nielsen

Electronic Systems Design, Specialization Project

Submission date: December 2019

Supervisor: Trond Ytterdal, IET

Co-supervisor: Carsten Wulff, IET

Norwegian University of Science and Technology

Department of Electronic Systems

Abstract.

An open source Python-language design automation and simulation framework for the design of integer-N all digital phase locked loop (ADPLL) frequency synthesizers is presented in this paper. The framework enables (1) automatic design of optimized second order discrete time digital loop filters, and (2) behavioral ADPLL simulation to verify loop filter and PLL designs for satisfactory phase noise, lock-time and stability; optionally subject to variation using Monte-Carlo sampling. Simulation is implemented with a discrete-event time domain simulator utilizing behavioral PLL component models, permitting accurate modeling of effects of time-discretization and quantization in an ADPLL. Loop filter design automation is based upon a prototype second order filter, whose parameters are optimized to minimize total integrated output phase noise for a PLL provided specifications for reference frequency, divider ratio, time-to-digital converter (TDC) resolution, digitally controlled oscillator (DCO) gain, oscillator phase noise characteristics and maximum lock time. The optimizer utilizes continuous phase transfer function approximation of ADPLL dynamics and phase noise, which allows for computationally fast evaluation, but also requires conversion of the design filters from continuous-to-discrete time. Second order optimization is utilized post filter design to map the discrete filter into a fixed-point digital with acceptable quantization noise and filter error due to quantization effects.

Problem description.

The intent of this project is to develop a standalone PLL design and simulation framework to aid and facilitate a later master's thesis project regarding the design of an all-digital, ultra-low power PLL frequency synthesizer. This framework is intended to address and ease all-digital PLL design and simulation challenges at a high level. Specifically it should enable speedy PLL simulation defined with system and component- level specifications (e.g. desired frequency, gain of digitally controlled oscillator, phase detector resolution, divider ratio). This is to allow for development of component level specifications and verification of PLL performance (phase noise, lock time, stability) under ideal circumstances before transistor level implementation, thus accelerating overall implementation time for hardware.

Contents

1 Introduction **10**

2 Theory **12**

2.1 Continuous PLL Model . . . 13
2.1.1 PLL Synthesizer architecture . . . 13
2.1.2 Divider . . . 13
2.1.3 Phase detector . . . 13
2.1.4 Loop Filter . . . 14
2.1.5 VCO . . . 14
2.1.6 Continuous PLL Transfer function . . . 14
2.2 ADPLL - digital, discretized PLL Model . . . 15
2.2.1 Divider . . . 15
2.2.2 TDC . . . 16
2.2.3 Discrete-time loop filter . . . 17
2.2.4 DCO . . . 18
2.2.5 Discrete-time PLL transfer function . . . 18
2.3 ADPLL Noise Model . . . 19
2.3.1 TDC noise . . . 19
2.3.2 DCO noise . . . 20
2.3.3 Divider noise . . . 21
2.3.4 Loop filter noise - direct form I . . . 22
2.3.5 PLL noise sensitivity transfer functions . . . 23
2.3.6 PLL phase signal and output PSD relationship for noise . . . 24
2.3.7 PLL output-referred noise PSD . . . 25

3 Loop Filter Design Automation **27**

3.1 Design sequence . . . 27
3.2 Loop filter Prototype . . . 28
3.2.1 Continuous PI-loop filter design . . . 29
3.2.2 PI-controller peaking compensation . . . 31
3.2.3 Alternative PID controller permutations . . . 31
3.2.4 Discretized Loop Filter Prototype . . . 32
3.2.5 Prototype PLL response . . . 32

4 Behavioral ADPLL simulation **34**

4.1 Simulation engine . . . 34
4.2 Clock behavioral model . . . 35
4.3 TDC behavioral model . . . 36

4.4 Loop filter behavioral model 36
4.5 DCO behavioral model 37
4.6 Divider behavioral model 38
4.7 Post processing: lock time detection 39
4.8 Post processing: phase noise power spectrum estimate 39
4.9 Monte-Carlo sampling 40

5 Loop filter optimization 41
5.1 Fast estimation of PLL settling time 41
5.2 Estimation of PLL phase noise 42
5.3 Loop filter optimization algorithm 43
5.4 Loop filter optimization - finite word effects 44

6 Discussion and results 45
6.1 Divider noise constraint 46
6.2 Example exercise 47

7 Conclusion 48

A Oscillator phase noise due to thermal noise 50

List of Figures

1 Basic phase feedback network. . . . 12
2 Basic PLL. . . . 13
3 Basic ADPLL. . . . 15
4 Digital divider signals. . . . 16
5 TDC model. . . . 16
6 Direct form I implementation of IIR filter. . . . 18
7 Discrete time PLL model. . . . 19
8 TDC quantization noise models. . . . 20
9 Quantization as via additive error signal. . . . 20
10 **(a)** Leeson model for phase noise, **(b)** DCO additive noise model. . . . 21
11 **(a)** Divider noise model, **(b)** Digital divider output jitter. . . . 21
12 Direct form I filter implementation with quantization. . . . 23
13 Full PLL additive noise model. . . . 24
14 Filter design sequence. . . . 27
15 PI-controller PLL pole-zero locations. . . . 30
16 Example PI-PLL responses with varied ζ. . . . 30
17 Implementation of filter. . . . 32
18 Simulation process. . . . 34
19 Discrete model for oscillator random walk. . . . 38
20 DCO additive noise model. . . . 50
21 Voltage to phase noise conversion. . . . 50

List of Tables

1 System-level specifications . . . 47
2 Component-level specifications. . . . 47

Abbreviations.

ADPLL	All digital phase locked loop
BER	Bit error rate
BFGS	Broyden-Fletcher-Goldfarb-Shanno
BW	Bandwidth
CMOS	Complementary metal oxide semiconductor
DCO	Digitally controlled oscillator
DIV	Divider
DNL	Differential non-linearity
FFT	Fast Fourier transform
FM	Frequency modulation
IIR	Infinite impulse response
ISM	Industrial, scientific and medicine
LF	Loop filter
LSB	Least signigicant bit
OTW	Oscillator tuning word
PD	Phase detector
PI	Propotional-integral
PID	Proportional-integral-derivative
PLL	Phase locked loop
PN	Phase noise
PSD	Power spectral density
PVT	Process, voltage and temperature
RMS	Root mean squared
SSB	Single side band
TDC	Time to digital converter
TF	Transfer function
VCO	Voltage controlled oscillator

1 Introduction

Phase locked loops are extraordinarily useful frequency synthesizers that are vital to the operation of virtually all wired and wireless communication systems of today. The trend towards increasingly lower power wireless devices poses an acute need to reduce PLL power consumption. This is a challenge as PLLs typically rank among the highest power consuming components of a radio, and are necessarily so to limit oscillator phase noise. Reducing analog PLL power consumption can be a prohibitive challenge as the performance of analog loop filters degrade as a result of unavoidably lower charge pump current. However, recent CMOS process nodes with minimum gate lengths as small as 7nm allow for all-digital PLLs as an attractive alternative to analog designs due to low power consumption associated with the implementation of a digital loop filter. Digital loop-filters have the unique advantage where they can be scaled indefinitely as process nodes advance, suffering no loss in performance, while also having greatly reduced sensitivities to process, voltage, temperature (PVT) variations compared to analog implementations.

All-digital PLLs introduce new challenges in the process of design in the ultra-low power domain. Low power design is complemented by low complexity design, which in a PLL transcribes to low resolution of phase detectors, digitally tunable oscillators, and loop filter digital data paths. In other words, effects of quantization are strong. Quantization is an inherently non-linear process, thus strong quantization is tied to strong non-linear effects. Consequently, where high resolution digital PLLs with low quantization effects can be effectively analyzed with linear-time invariant transfer functions in the Z-domain, simulation and numerical analysis is necessary to accurately capture quantization effects in low power, low resolution ADPLLs . This, of course, presents a challenge in manual loop filter design of PLLs if simulation is an integral part to the most basic modeling, and thus motivates the creation of an automated design solution. Currently, no PLL design framework currently automates PLL loop filter design for the needs of ultra low power digital PLLs as characterized here.

Thus in this paper, a new framework written in pure-Python is introduced, which uniquely addresses issues of ultra-low power ADPLL design. Specifically, design of integer-N type PLLs is focused on, as the impetus of this work is an integer-N PLL design project. Topics presented are (a) automatic design and optimization of ADPLL loop filters given target system and component level specifications for the PLL, and (b) behavioral time domain PLL simulation for accurate analysis and verification of loop filter and PLL performance, with an integrated Monte-Carlo sampling variation analysis engine.

A brief outline of the paper is as follows. An introduction to PLL theory is in section 2. Simulation and optimization methods are discussed in sections 3-5. An example design

exercise, a comparison to existing solutions, and general discussion considerations for using the framework are in section 6. Finally, section 7 concludes.

The main contributions of this work to PLL design are:

1. Fully automatic ADPLL loop filter design and optimization for all digital PLLs based on high level PLL specifications in an open source framework.
2. Integrated behavioral time domain simulation of integer-N digital PLLs for verification of filter and PLL design, with variational analysis of performance and stability.

2 Theory

In its most basic form, a phase locked loop is a phase-based feedback system whose output tracks or maintains a fixed phase relationship to an input signal. As will be shown, such a system is uniquely suited to the task of frequency synthesis, which is the process of generating derivative frequencies from some reference frequency. Given reference and output phase signals Φ_{ref} and Φ_{out}, a PLL can be modeled as in figure 1, with feedforward and feedback networks A(s) and B(s).

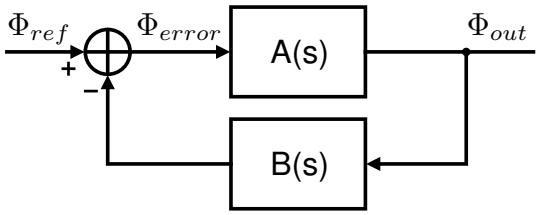

Figure 1: Basic phase feedback network.

The closed loop phase response T(s) for Φ_{ref} to Φ_{out} is therefore:

$$\mathrm{T}(s) = \frac{\Phi_{out}(s)}{\Phi_{ref}(s)} = \frac{A(s)}{1 + A(s)B(s)} \tag{1}$$

A particular case of interest is when B(s) = 1/N, where N is a constant, and the loop gain L(s) = A(s)B(s) $>>$ 1. The closed loop response for this case is:

$$\frac{\Phi_{out}(s)}{\Phi_{ref}(s)} \approx \frac{A(s)}{A(s)B(s)} = \frac{1}{B(s)} = N \tag{2}$$

We see that the phase through the PLL is multiplied by a factor of N. If the input phase signal is a sinusoid with frequency ω_{ref}, and likewise the output with ω_{out}, then $\phi_{ref}(t) = \omega_{ref}t$ and $\phi_{out}(t) = \omega_{out}t$. Thus:

$$\frac{\Phi_{out}(t)}{\Phi_{ref}(t)} = \frac{\omega_{out}t}{\omega_{ref}t} \approx N \quad \rightarrow \quad \omega_{out} \approx N\omega_{ref} \tag{3}$$

Therefore, it is observed that a PLL allows for the generation, i.e. synthesis, of a new frequency from a reference frequency signal. Given a feedback divider ratio of 1/N, the PLL multiplies the reference frequency by a factor of N. In the following sections, more advanced models for PLL will be developed, extending the concept introduced here. Specifically, the theory of digital, discrete-time PLLs will be developed and extended from a continuous phase model of a basic PLL.

2.1 Continuous PLL Model

Although this work is interested in discrete time sampling PLL design, as will later be seen continuous models can still be of use in the analysis and design of such systems. Thus a continuous PLL model is developed in this section.

2.1.1 PLL Synthesizer architecture

The traditional architecture for implementing a PLL frequency synthesizer [12] is shown in figure 2. This basic PLL is comprised of four components: (1) a phase detector, denoted by PD, (2) a loop filter, denoted by $\mathrm{H}_{LF}(\mathrm{s})$, (3) a voltage controlled oscillator, denoted by VCO, and (4) and phase divider, denoted by "÷ N" in the figure. These components are explained in the following sections.

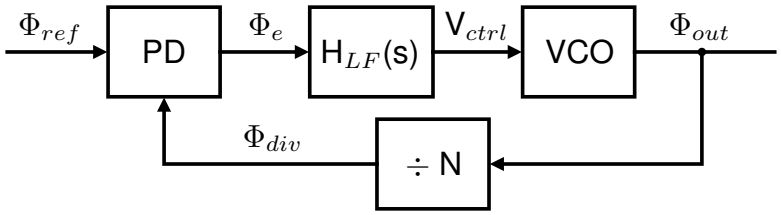

Figure 2: Basic PLL.

2.1.2 Divider

The phase divider is used as the feedback path in the PLL, where the division ratio N controls the phase and consequent frequency multiplication of the PLL. The tranfer function of the divider is:

$$\mathrm{H}_{div}(s) = \frac{\Phi_{div}(s)}{\Phi_{out}(s)} = \frac{1}{\mathrm{N}} \tag{4}$$

2.1.3 Phase detector

The phase detector is used to measure the phase of the feedback signal (i.e. divider output) in relation to the reference phase, in order to establish a phase error signal Φ_e used to control the tuning of the PLL.

$$\Phi_e(s) = \Phi_{ref}(s) - \Phi_{div}(s) \tag{5}$$

2.1.4 Loop Filter

The PLL loop filter is used to control the phase-frequency response of PLL, which affects transient PLL behavior, as well as phase noise performance (see section 2.3). This can be designed to have P poles and Z zeros, and can be represented in the canonical form of equation 6 as a rational function of polynomials of s with coefficients given with $\{a_0, ..., a_P\}$ and $\{b_0, ..., b_Z\}$.

$$\mathrm{H}_{LF}(s) = \frac{\sum_{j=0}^{Z} b_j s^j}{\sum_{k=0}^{P} a_k s^k} \tag{6}$$

2.1.5 VCO

The voltage controlled oscillator is an oscillator with frequency controlled by an input signal V_{ctrl}. The VCO is characterized by its gain $K_{DCO} = \partial f / \partial \mathrm{V}_{ctrl}$, and the nominal oscillation frequency f_0. Analyzed in terms of phase, an oscillator can be seen as a time-phase integrator:

$$\Phi_{VCO}(t) = \Phi_{out}(t) = \int 2\pi(K_{DCO}\mathrm{V}_{ctrl}(t) + f_0)\mathrm{dt} \tag{7}$$

In the s-domain, where frequency offsets will be represented via initial conditions for modeling purposes, the VCO transfer function is therefore:

$$\mathrm{H}_{VCO}(s) = \frac{\Phi_{VCO}(s)}{\mathrm{V}_{ctrl}(s)} = \frac{\Phi_{out}(s)}{\mathrm{V}_{ctrl}(s)} = \frac{2\pi K_{DCO}}{s} \tag{8}$$

2.1.6 Continuous PLL Transfer function

Now that the continuous PLL synthesizer is understood at a component level, the closed loop dynamics of the PLL can be analyzed. First the PLL loop gain is determined:

$$\mathrm{L}(s) = \mathrm{H}_{LF}(s)\mathrm{H}_{VCO}(s)\mathrm{H}_{div}(s) = \frac{2\pi K_{VCO}}{\mathrm{N}} \frac{1}{s} \frac{\sum_{j=0}^{Z} b_j s^j}{\sum_{k=0}^{P} a_k s^k} \tag{9}$$

With the phase detector as the feedback summation point, the closed loop response of the PLL from reference to output is in equation 10.

$$\mathrm{T}(s) = \frac{\Phi_{out}(s)}{\Phi_{ref}(s)} = \frac{2\pi K_{VCO} \sum_{j=0}^{Z} b_j s^j}{\sum_{k=0}^{P} a_k s^{k+1} + \frac{2\pi K_{VCO}}{\mathrm{N}} \sum_{j=0}^{Z} b_j s^j} = \mathrm{N}\frac{\mathrm{L}(s)}{1 + \mathrm{L}(s)} \tag{10}$$

2.2 ADPLL - digital, discretized PLL Model

Based on the continuous PLL theory, a model for digital, discrete time sampled PLLs (i.e. ADPLLs) can be adapted. The general approach here is to utilize the bilinear transformation between continuous s-domain models to the discrete z-domain models and vice-versa. As commonly cited in PLL literature from a seminal paper by Gardner [3], if the PLL sampling frequency $f_s > 10 \cdot \mathrm{BW}_{loop}$, where BW_{loop} is the PLL loop bandwidth, the granularity effects due to time-sampling can be neglected. Thus the design methods established in this paper are predicated on $f_s > 10 \cdot \mathrm{BW}_{loop}$.

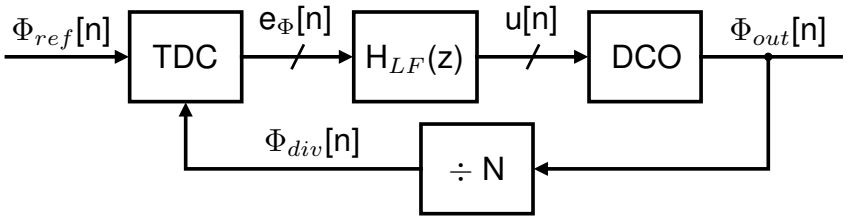

Figure 3: Basic ADPLL.

The basic architecture of an ADPLL is shown in figure 3. Here, compared to the continuous PLL of figure 2, the phase detector has been replaced with a time to digital converter (TDC), the loop filter $\mathrm{H}_{LF}(s)$ with a discrete-time loop filter $\mathrm{H}_{LF}(z)$, and the VCO with a digitally controlled oscillator (DCO). In this architecture, all components are fully or partially digital in implementation.

2.2.1 Divider

A digital divider functions by counting input cycles. With a divider modulus N, the output of the divider will have an active edge transition (considered to be rising edge as shown in figure 4) every N-cycles. Phase information is inferred from active edge timing, which occurs with time interval N/f_{osc}, and is equal to the point at which output phase equals a multiple of 2π. Thus a digital divider does not provider continuous phase information, but rather a sampled phase signal with rate f_{osc}/N.

For PLL transfer function modeling, a digital divider behaves identically to the continuous case:

$$\Phi_{div}[n] = \frac{\Phi_{out}[n]}{\mathrm{N}} \tag{11}$$

Application of the z- and s-domain transformations:

$$\mathrm{H}_{div}(z) = \mathrm{H}_{div}(s) = \frac{\Phi_{div}(z)}{\Phi_{out}(z)} = \frac{1}{\mathrm{N}} \tag{12}$$

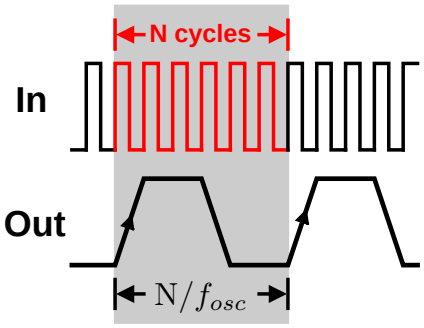

Figure 4: Digital divider signals.

2.2.2 TDC

The TDC is a digital, quantized representation of the the phase detector. It takes input phase signals Φ_{div}[n] and Φ_{ref}[n], and outputs a digital phase error word $e_\Phi[n]$. Figure 5 shows the basic TDC model architecture. Being digitized, a TDC will have limited resolution in phase, equivalent to M steps per reference cycle. This is a minimum step size in time of Δt_{step} = $1/Mf_{ref}$. Since the output of the TDC is digital, the model applies a scale factor M/2π and floor rounding, so 1 least significant bit (LSB) of $e_\Phi[n]$ equates to Δt_{step} timing error between Φ_{div}[n] and Φ_{ref}[n].

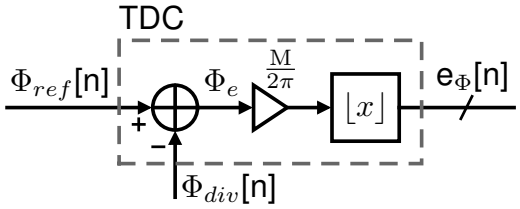

Figure 5: TDC model.

In sampled-time equation form:

$$e_\Phi[n] = \left\lfloor \frac{\mathrm{M}}{2\pi}(\Phi_{ref}[n] - \Phi_{div}[n]) \right\rfloor \tag{13}$$

For purposes of PLL loop gain calculation, the TDC z- and s-domain representation is equation 15, which accounts for phase-to-digital domain conversion gain. Effects of quantization will be handled in section 2.3.

$$e_\Phi(z) = \frac{\mathrm{M}}{2\pi}(\Phi_{ref}(z) - \Phi_{div}(z)) \tag{14}$$

$$\mathrm{H}_{TDC}(z) = \mathrm{H}_{TDC}(s) = \frac{\mathrm{M}}{2\pi} \tag{15}$$

2.2.3 Discrete-time loop filter

The discrete-time loop filter design will be derived from the continuous canonical loop filter (equation 6) via application of a s-to-z domain transformation. The bilinear transform [11] allows for such conversion from continuous transfer function to discrete representation. However, in the case presented in this work, where a high degree of sampling ($f_s > 10 \cdot \mathrm{BW}_{loop}$) is employed, a simpler transformation is permissable, derived through Taylor series approximation of z=$re^{s\Delta T}$ for values on the unit circle, i.e. r=1. This will be refered to as the approximate bilinear transform in this work. Given the $1/\Delta T_s$=f_{ref} as the relation for sampling rate, then:

$$\begin{aligned} z^{-1} &= e^{-s\Delta T_s} && \text{(definition of z-space on unit circle)} \\ &= \sum_{k=0}^{\infty} \frac{(-s\Delta T_s)^k}{k!} && \text{(exponential Taylor series)} \\ &\approx 1 - s\Delta T_s && \text{(if } |s\Delta T_s| = 2\pi \mathrm{BW}_{loop} \cdot \Delta T_s << 1) \end{aligned}$$

Thus the s-to-z and z-to-s identities for the approximated bilinear transform are:

$$z^{-1} = 1 - s\Delta T_s \tag{16}$$

$$s = \frac{1}{\Delta T_s}(1 - z^{-1}) \tag{17}$$

Applying 17 to equation 6 yields the z-domain loop filter:

$$\mathrm{H}_{LF}(z) = \mathrm{H}_{LF}(s)|_{s=\frac{1}{\Delta T_s}(1-z^{-1})} = \left.\frac{\sum_{j=0}^{Z} b_j s^j}{\sum_{k=0}^{P} a_k s^k}\right|_{s=\frac{1}{\Delta T_s}(1-z^{-1})} \tag{18}$$

$$= \frac{\sum_{j=0}^{Z} b_j (1 - z^{-1})^j}{\sum_{k=0}^{P} a_k (1 - z^{-1})^k} \tag{19}$$

Equation 19 is transformed to a digitally implementable representation by reorganizing into the canonical representation of 20, which then determines the tap coefficients for the sampled-time difference equation 21.

$$\mathrm{H}_{LF}(z) = \frac{\sum_{j=0}^{P} b_j' z^{-j}}{1 + \sum_{k=1}^{Z} a_k' z^{-k}} \tag{20}$$

$$y[n] = -\sum_{k=1}^{P} a_k' y[n-k] + \sum_{j=0}^{Z} b_j' x[n-j] \tag{21}$$

The obtained difference equation is directly implementable in digital hardware with a direct from I IIR filter [10] shown in figure 6. The filter coefficients $\{a_1', ..., a_P'\}$ and $\{b_0', ..., b_Z'\}$ must be quantized into finite resolution fixed point words for a complete digital implementation.

The delay elements (z^{-1} blocks) are implementable digitally as registers, the coefficient gains are implementable with array multipliers and the adders are implementable with digital adders. Effects of quantization will be discussed in section 2.3.

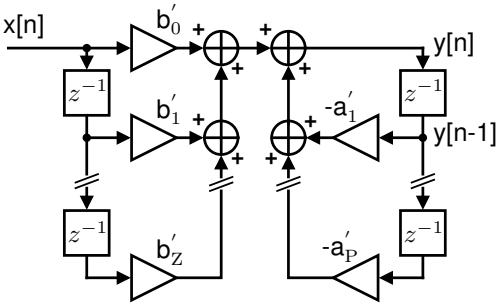

Figure 6: Direct form I implementation of IIR filter.

2.2.4 DCO

The digitally controlled oscillator varies from a VCO by only accepting a digital frequency tuning signal, called the oscillator tuning word (OTW). A DCO modeled in discrete time as a recursive phase integrator, dependent on (a) the DCO gain K_{DCO}, equal to the frequency tuning of the oscillator per LSB of the OTW, (b) the current state of the OTW u[n], and (c) the PLL sampling period T=f_{ref}^{-1}.

$$\Phi_{out}[n] = \Phi_{out}[n-1] + 2\pi K_{DCO} u[n] \Delta T_s \tag{22}$$

Application of the z-transform yields:

$$\mathrm{H}_{DCO}(z) = \frac{\Phi_{out}(z)}{u(z)} = \frac{2\pi K_{DCO} \Delta T_s}{1 - z^{-1}} \tag{23}$$

Application of the bilinear transform to the DCO transfer function yields:

$$\mathrm{H}_{DCO}(s) = \frac{\Phi_{out}(s)}{u(s)} = \frac{2\pi K_{DCO} \Delta T_s}{1 - (1 - s\Delta T_s)} = \frac{2\pi K_{DCO}}{s} \tag{24}$$

2.2.5 Discrete-time PLL transfer function

The transfer function for the discrete-time PLL of figure 7 can be computed in the z-domain, and also approximated continuously. The open loop z-domain transfer function is:

$$\mathrm{L}(z) = \mathrm{H}_{TDC}(z)\mathrm{H}_{LF}(z)\mathrm{H}_{DCO}(z)\mathrm{H}_{DIV}(z) = \frac{\mathrm{M}}{\mathrm{N}} \frac{K_{DCO}\Delta T_s}{(1 - z^{-1})} \frac{\sum_{j=0}^{Z} b_j (1 - z^{-1})^j}{\sum_{k=0}^{P} a_k (1 - z^{-1})^k} \tag{25}$$

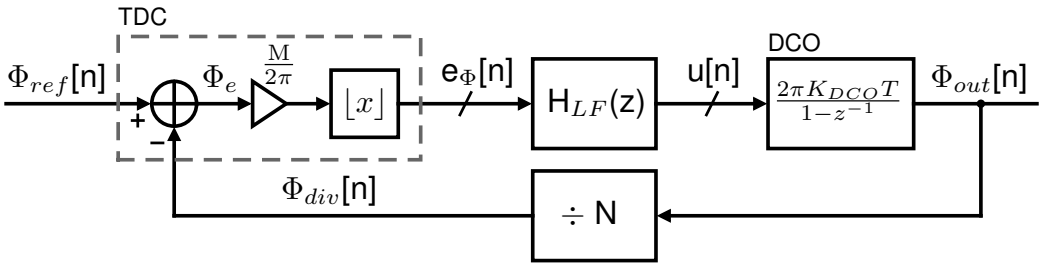

Figure 7: Discrete time PLL model.

The closed loop z-domain PLL phase transfer function is:

$$\mathrm{T}(z) = \frac{\Phi_{out}(z)}{\Phi_{ref}(z)} = \frac{\mathrm{M}K_{DCO}\Delta T_s \sum_{j=0}^{Z} b_j (1-z^{-1})^j}{\sum_{k=0}^{P} a_k (1-z^{-1})^{k+1} + K_{DCO}\Delta T_s \frac{\mathrm{M}}{\mathrm{N}} \sum_{j=0}^{Z} b_j (1-z^{-1})^j} \tag{26}$$

The s-domain approximation of the transfer function is:

$$\mathrm{L}(s) = \mathrm{H}_{TDC}(s)\mathrm{H}_{LF}(s)\mathrm{H}_{DCO}(s)\mathrm{H}_{DIV}(s) = \frac{\mathrm{M}}{\mathrm{N}} \frac{K_{DCO}}{s} \frac{\sum_{j=0}^{Z} b_j s^j}{\sum_{k=0}^{P} a_k s^k} \tag{27}$$

And in closed loop configuration the s-domain PLL phase transfer function is:

$$\mathrm{T}(s) = \frac{\Phi_{out}(s)}{\Phi_{ref}(s)} = \frac{\mathrm{M}K_{DCO} \sum_{j=0}^{Z} b_j s^j}{\sum_{k=0}^{P} a_k s^{k+1} 1 + \frac{\mathrm{M}}{\mathrm{N}} K_{DCO} \sum_{j=0}^{Z} b_j s^j} = \mathrm{N}\frac{\mathrm{L}(s)}{1+\mathrm{L}(s)} \tag{28}$$

2.3 ADPLL Noise Model

The noise in the discrete-time ADPLL result from quantization and from stochastic sources. Quantization results from round off errors introducted in the digitization of PLL components (in the TDC, loop filter, and DCO). Stochastic noise results from thermal and flicker noise in the PLL components when considered in an analog viewpoint (present in the DCO, divider and TDC). The noise generated by these quantization sources will be discussed in the following sections, based on a modeling and noise analysis approach from [9].

2.3.1 TDC noise

The predominant phase noise source in the TDC is due to quantization. A straightforward approach to model quantization noise is to utilize the model of figure 8b to represent quantization.

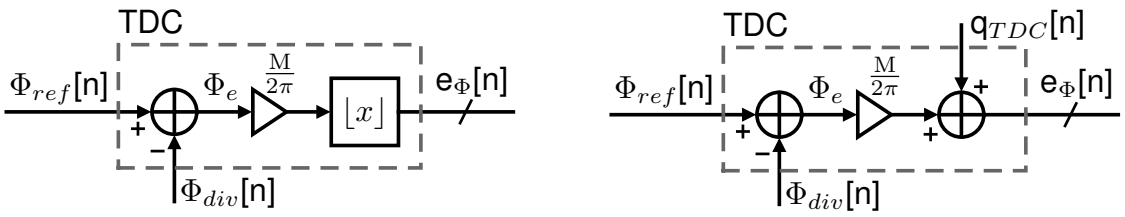

(a) TDC Model. **(b)** TDC additive noise model.

Figure 8: TDC quantization noise models.

Using this model, the quantized signal e_Φ[n] is the sum of the its unquantized representation $\Phi_e \frac{M}{2\pi}$ with a quantization error signal $q_{TDC}[n]$. Figure 9 illustrates this process.

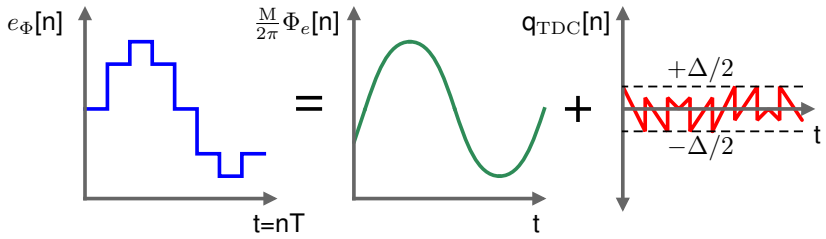

Figure 9: Quantization as via additive error signal.

The quantization noise signal has the statistical property that it is uniformly distributed in the range $[-\Delta/2, \Delta/2]$, i.e. $P_q(Q = q) = \mathrm{U}(-\Delta/2, \Delta/2)$ if Δ is the quantization step size. The power of the TDC quantization noise signal is:

$$\sigma^2_{q_{TDC}} = \int_{-\infty}^{\infty} q^2 P_q(Q = q) dq = \int_{-\Delta/2}^{\Delta/2} \frac{q^2}{\Delta} dq = \frac{\Delta^2}{12} \tag{29}$$

Since e_Φ[n] is digital signal, the minimum step size is Δ=1 LSB. The TDC quantization noise power is therefore $\sigma^2_{q_{TDC}} = 1/12$ LSB^2. The po If the quantization noise is assumed to be white, and the TDC is sampled at f_{ref}, the quantization PSD is:

$$S_{qn_{TDC}}(f) = \frac{P_{q_{TDC}}}{\Delta f} = \frac{\sigma^2_{q_{TDC}}}{f_{ref}} = \frac{\Delta^2}{12 f_{ref}} = \frac{1}{12 f_{ref}} \quad \frac{[\mathrm{LSB}]^2}{[\mathrm{Hz}]} \tag{30}$$

2.3.2 DCO noise

Noise in a DCO is resulting from (a) quantization of the oscillator tuning word u[n], and (b) from thermal and stochastic sources. In the digital PLL, the OTW quantization occurs in the loop filter, so this will be analyzed in the later loop filter section (2.3.4). Thus oscillator thermal/stochastic noise will be considered, based on Leeson's model for oscillator phase noise [6]. Leeson's model considers noise power density at an offset Δf from the oscillator tone (carrier). Noise power density is represented with the function $\mathcal{L}(\Delta f)$, which is the noise

power density normalized to the power of the oscillator carrier tone, in other words in units of dBc/Hz. Leeson's model divides phase noise into three regions, illustrated in figure 10a: (1) flicker-noise dominated, with a slope of -30 dB/decade, (2) white frequency-noise dominated, with -20 dB per decade, and (3) a flat region, limited by the thermal noise floor or amplitude noise. It is noted that phase noise components are at frequencies different than the carrier, hence are orthogonal, and can be treated as independent components that are added to the main carrier frequency for analysis. Figure 10b demonstrates the application of this principle for modeling of the DCO phase noise $\Phi_{n_{DCO}}$ as an additive process to the oscillator phase Φ_{osc}, thus $\Phi_{out} = \Phi_{osc} + \Phi_{n_{DCO}}$.

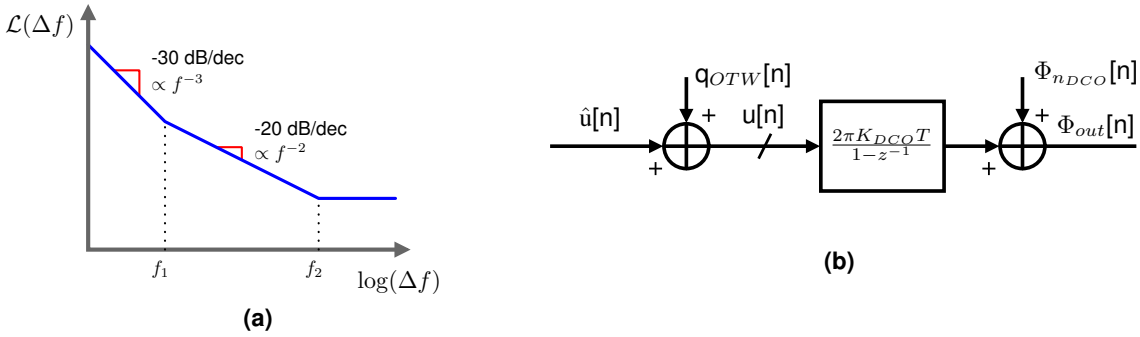

Figure 10: (a) Leeson model for phase noise, **(b)** DCO additive noise model.

The equation for $\mathcal{L}(\Delta f)$ (from [5]) is in 31, and is dependent on the temperature T, excess noise factor F, oscillator power P, oscillator Q factor, and the transition frequencies f_1 and f_2 that separate the different noise regions. It is of interest to note that the phase noise relative to the carrier will increase as power decreases, which provides challenge for creating low power oscillators with acceptable phase noise characteristics.

$$\mathcal{L}(\Delta f) = 10\log_{10}\left[\frac{2\mathrm{F}k_B\mathrm{T}}{\mathrm{P}}\left(1+\left(\frac{f_2}{2Q\Delta f}\right)^2\right)\left(1+\frac{f_1}{|\Delta f|}\right)\right] = S_{\Phi n_{DCO}}(\Delta f) \tag{31}$$

For notational consistency, the following redefinition is used in the remainder of this paper: $S_{\Phi n_{DCO}}(f) = \mathcal{L}(\Delta f)|_{\Delta f = f}$

2.3.3 Divider noise

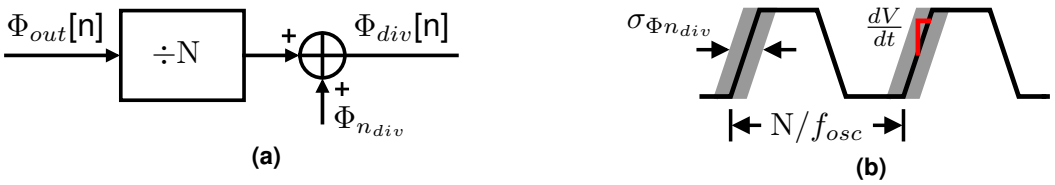

Figure 11: (a) Divider noise model, **(b)** Digital divider output jitter.

Divider noise is manifested as jitter (with RMS distribution in time of $\sigma_{tn_{div}}$) on the the divider output. This is due to effects of stochastic and uncorrelated voltage noise coupling into the

signal phase, much like in the case of oscillator phase noise. If the divider is a digital circuit, with edge rate dV/dt, and subject to thermal noise in the form of a voltage v_n, with noise power of $\sigma^2_{v_n}$, the divider phase noise power added to the divider output is:

$$\sigma^2_{\Phi n_{div}} = \omega^2_{ref}\sigma^2_{tn_{div}} = \omega^2_{ref}\left(\frac{dV}{dt}\right)^{-2}\sigma^2_{v_n} \tag{32}$$

At lock, the output of a digital divider will have an update rate $f_{osc}/\mathrm{N} \approx f_{ref}$, which can be treated as the sampling rate of the output phase signal $\Phi_{div}[n]$. Thus if the divider phase noise power is confined into a bandwidth equal to f_{ref}, the spectral density of divider noise is:

$$S_{\Phi n_{div}}(f) = \frac{\sigma^2_{\Phi n_{div}}}{f_{ref}} = 2\pi\omega_{ref}\sigma^2_{tn_{div}} = 2\pi\omega_{ref}\left(\frac{dV}{dt}\right)^{-2}\sigma^2_{v_n} \quad \frac{[\mathrm{rad}]^2}{[\mathrm{Hz}]} \tag{33}$$

2.3.4 Loop filter noise - direct form I

In a digital loop filter, quantization noise arises from rounding errors due to finite precision in the arithmetic circuits that implement the filter. Quantization noise power here will be derived under the assumption of a direct form I filter implementation, with B bits in each fixed point word throughout the loop filter. In a digital implementation of the canonical z-domain transfer function 34 as the direct form I structure of figure 12a, delays are constructed using registers, adders with digital adders, and the filter coefficient gain terms $\{a_1, ...a_N; b_0, ..., b_M\}$ with digital multipliers. The registers and adders do not introduce extra round-off error beyond that already existing (if overflows do not occur). However, the multipliers will if the products resulting from two B bit words (nominally 2B bits), are mapped back onto B bit words.

$$\mathrm{H}_{LF}(z) = \frac{\sum_{j=0}^{Z} b_j z^{-j}}{1 + \sum_{k=1}^{P} a_k z^{-k}} \tag{34}$$

Quantization in this case can be represented by adding a quantization error signal q_x[n] to the result of each ideal multiplication, as shown in figure 12b. This is the same approach for TDC quantization noise in section 2.3.1. The noise power associated with each q_x[n] is identical, with $\sigma^2_{qx} = 1/12\ \mathrm{LSB}^2$.

Assuming the quantization error signals of each multiplier are uncorrelated with all other multipliers, the output-referred noise power of the filter can be computed as the sum of the output-referred individual contributions. These contributions can be determined via solving for the transfer function from each source q_x[n] of each quantization noise to the output y[n]. In the case of the direct form I filter structure, all quantization sources q_x[n] have the same

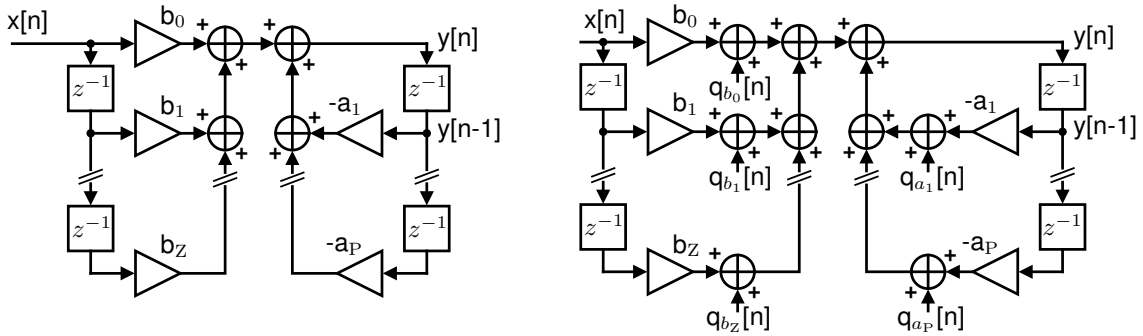

(a) Ideal structure. **(b)** With added quantization error signals.

Figure 12: Direct form I filter implementation with quantization.

transfer characteristic to the output y[n] given in 35.

$$\frac{Y(z)}{Q_x(z)} = \frac{1}{1 + \sum_{k=1}^{P} a_k z^{-k}} \tag{35}$$

Applying the bilinear transform to 35, with high oversampling where N·BW$_{loop}$10 $< f_{ref}$, and N is the number of poles in the system.

$$\left.\frac{Y(z)}{Q_x(z)}\right|_{z^{-1}=1-sT} \approx \frac{1}{1 + \sum_{k=1}^{P} a_k - s\sum_{k=1}^{P} k a_k} \tag{36}$$

The output power spectral density is then for one error source is, confined to a bandwidth defined by the (sampling) reference frequency f_{ref}:

$$S_{qx}(f) = \frac{\sigma_{qx}^2}{f_{ref}} \left|\frac{Y(s)}{Q_x(s)}\right|^2_{s=j2\pi f} \approx \frac{1}{12 f_{ref}} \left|\frac{1}{1 + \sum_{k=1}^{P} a_k - j2\pi f \sum_{k=1}^{P} k a_k}\right|^2 \quad \frac{[\text{LSB}]^2}{[\text{Hz}]} \tag{37}$$

Given P poles and Z zeros in the filter, the total output quantization PSD of the filter is 38. The total loop filter noise PSD linearly scales with the number of multipliers in the direct form I filter implementation.

$$S_{qn_{LF}}(f) = (P + Z + 1) S_{qx}(f) \quad \frac{[\text{LSB}]^2}{[\text{Hz}]} \tag{38}$$

2.3.5 PLL noise sensitivity transfer functions

Having developed models for noise of generated by each PLL component, noise sensitivity transfer functions must be computer to refer each noise source to the PLL output in terms of phase. In the developed noise theory, thus far all noise sources have been modeled as additive phase components. The full system model illustrating this is in figure 13.

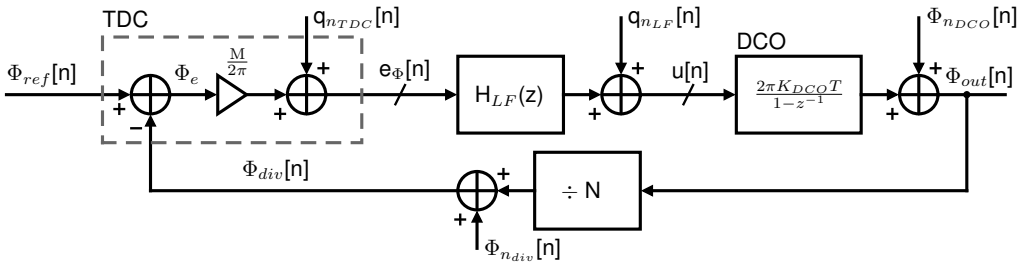

Figure 13: Full PLL additive noise model.

Following the approach of [9], it is useful to define a transfer function $\hat{\mathrm{T}}(s)$ which characterizes the normalized closed loop response from reference to output of the PLL. $\hat{\mathrm{T}}(s)$ is defined in terms of the loop gain L(s).

$$\hat{\mathrm{T}}(s) = \frac{\mathrm{L}(s)}{1+\mathrm{L}(s)} \quad \text{s.t.} \quad \mathrm{T}(s) = \frac{\Phi_{out}}{\Phi_{ref}} = \mathrm{N}\hat{\mathrm{T}}(s) \tag{39}$$

Solving for the closed transfer functions between each $q_{n_{TDC}}$, $q_{n_{LF}}$, $\Phi_{n_{DCO}}$ and $\Phi_{n_{div}}$ to the output Φ_{out} utilizing s-domain approximations yields equations 40-43.

$$\frac{\Phi_{out}(s)}{q_{n_{TDC}}(s)} = \frac{2\pi\frac{K_{DCO}}{s}\mathrm{H}_{LF}(s)}{1+\mathrm{L}(s)} = 2\pi\frac{\mathrm{N}}{\mathrm{M}}\frac{\mathrm{L}(s)}{1+\mathrm{L}(s)} = 2\pi\frac{\mathrm{N}}{\mathrm{M}}\hat{\mathrm{T}}(s) \tag{40}$$

$$\frac{\Phi_{out}(s)}{\Phi_{n_{DCO}}(s)} = \frac{1}{1+\mathrm{L}(s)} = 1-\hat{\mathrm{T}}(s) \tag{41}$$

$$\frac{\Phi_{out}(s)}{q_{n_{LF}}(s)} = \frac{2\pi\frac{K_{DCO}}{s}}{1+\mathrm{L}(s)} = 2\pi\frac{K_{DCO}}{s}(1-\hat{\mathrm{T}}(s)) \tag{42}$$

$$\frac{\Phi_{out}(s)}{\Phi_{n_{div}}(s)} = \frac{\mathrm{M}\frac{K_{DCO}}{s}\mathrm{H}_{LF}(s)}{1+\mathrm{L}(s)} = \mathrm{N}\frac{\mathrm{L}(s)}{1+\mathrm{L}(s)} = \mathrm{N}\hat{\mathrm{T}}(s) \tag{43}$$

2.3.6 PLL phase signal and output PSD relationship for noise

When analyzing PLL noise, the noise power spectral density of the PLL output is of most interest. Up to this point, noise has been defined in terms of noise phase signal Φ_n, or an unwanted added component to the oscillator phase signal $\Phi_{osc} = \omega_{osc}t$. The PLL output phase signal Φ_{out} is thus:

$$\Phi_{out}(t) = \Phi_{osc}(t) + \Phi_n(t) = \omega_{osc}t + \Phi_n(t) \tag{44}$$

Computation of PSD requires the PLL output voltage waveforms. These here will be defined in terms of complex exponentials. Given an oscillation amplitude A_0:

$$V_{out} = \Re\left(A_0 e^{j\Phi_{out}(t)}\right) = \Re\left(A_0 e^{j\omega_{osc}t} e^{j\Phi_n(t)}\right) \tag{45}$$

Assuming the phase noise signal is zero mean, $\mathbb{E}[\Phi_n(t)] = 0$, and the power of phase noise signal is small, $\text{Var}[\Phi_n(t)] << 1$, then the approximation $e^{j\Phi_n(t)} = 1 + j\Phi_n(t)$ can be applied by truncating the exponential Taylor series expansion.

$$V_{out} = \Re\left(A_0 e^{j\omega_{osc}t} e^{j\Phi_n(t)}\right) = \Re\left(A_0 e^{j\omega_{osc}t} + j\Phi_n(t) A_0 e^{j\omega_{osc}t}\right) \tag{46}$$

$$= A_0 \cos(\omega_{osc}t) - \Phi_n(t) A_0 \sin(\omega_{osc}t) \tag{47}$$

The result is a carrier cosine signal, and an orthogonal sine signal modulated by the phase noise Φ_n. From this, the spectral density of the phase noise relative to the carrier can be estimated. The power spectral density $S_{V_{out}}$ is computed in 48-50. Due to orthogonality of the sine/cosine components of 47, the cross terms that appear in the PSD are zero.

$$S_{V_{out}}(f) = \lim_{\Delta T \to \infty} \frac{1}{\Delta T} |\mathcal{F}\{V_{out}(t) \cdot \text{rect}(t/\Delta T)\}|^2 \tag{48}$$

$$= \lim_{\Delta T \to \infty} \frac{A_0^2}{\Delta T} |\mathcal{F}\{\cos(\omega_{osc}t) \cdot \text{rect}(t/\Delta T)\}|^2 \tag{49}$$

$$+ \lim_{\Delta T \to \infty} \frac{A_0^2}{\Delta T} |\mathcal{F}\{\Phi_n(t) \cdot \text{rect}(t/\Delta T)\} * \mathcal{F}\{\sin(\omega_{osc}t) \cdot \text{rect}(t/\Delta T)\}|^2 \tag{50}$$

The noise power spectral density $\mathcal{L}(\Delta f)$ is defined as the noise PSD at offset Δf from the carrier frequency f_{osc}, normalized to the carrier power. Here the PSD carrier component is given by 49, and the noise component by 50. Shifting 50 by ω_{osc} and performing normalization for carrier power results in:

$$\mathcal{L}(\Delta f) = \lim_{\Delta T \to \infty} \frac{1}{\Delta T} |\mathcal{F}\{\Phi_n(t) \cdot \text{rect}(t/\Delta T)\}|^2 \Big|_{f=\Delta f} = S_{\Phi_n}(\Delta f) \tag{51}$$

Thus, the PLL output noise PSD relative to the carrier $\mathcal{L}(\Delta f)$ is equal to the PSD of the phase noise signal $\Phi_n(t)$, $S_{\Phi_n}(\Delta f)$, provided $\text{Var}[\Phi_n(t)] << 1$.

2.3.7 PLL output-referred noise PSD

In terms of analysis, PLL noise PSD referred to the PLL output is of most interest. Thus far the following have been established: (a) noise spectrum generated by each individual PLL component, (b) the PLL phase noise sensitivity functions, and (c) the relationship between PLL output PSD and output phase noise. Now these can be combined to provide a final result for full PLL output-referred noise PSD. An important assumption here is all noise sources are uncorrelated, so their independent noise power contributions may be summed to find the total noise PSD. The PLL output phase noise PSD for each noise source is simply found by multiplying magnitude squared of the respective noise sensitivity function with the noise

source PSD. Thus:

$$S_{\Phi n_{TDC,out}}(f) = S_{qn_{TDC}}(f) \left| \frac{\Phi_{out}(f)}{q_{n_{TDC}}(f)} \right|^2 = \frac{1}{12 f_{ref}} \left| 2\pi \frac{\mathrm{N}}{\mathrm{M}} \hat{\mathrm{T}}(f) \right|^2 \tag{52}$$

$$S_{\Phi n_{DCO,out}}(f) = S_{\Phi n_{DCO}}(f) \left| \frac{\Phi_{out}(f)}{\Phi_{n_{DCO}}(f)} \right|^2 = \frac{S_{0\Phi n_{DCO}}}{f^2} \left| 1 - \hat{\mathrm{T}}(f) \right|^2 \tag{53}$$

$$S_{\Phi n_{LF,out}}(f) = S_{qn_{LF}}(f) \left| \frac{\Phi_{out}(f)}{q_{n_{LF}}(f)} \right|^2 \approx \frac{K_{DCO}^2}{12 f_{ref} f^2} \left| \frac{1 - \hat{\mathrm{T}}(f)}{1 + \sum_{k=1}^{P} a_k - j2\pi f \sum_{k=1}^{P} k a_k} \right|^2 \tag{54}$$

$$S_{\Phi n_{div,out}}(f) = S_{\Phi n_{div}}(f) \left| \frac{\Phi_{out}(f)}{\Phi_{n_{div}}(f)} \right|^2 = f_{ref} \left| 2\pi \sigma_{tn_{div}} \mathrm{N} \hat{\mathrm{T}}(f) \right|^2 \tag{55}$$

The output SSB noise PSD at offset Δf relative to the carrier normalized to carrier power of PLL will be:

$$\mathcal{L}(\Delta f) = S_{\Phi n_{TDC,out}}(\Delta f) + S_{\Phi n_{DCO,out}}(\Delta f) + S_{\Phi n_{LF,out}}(\Delta f) + S_{\Phi n_{div,out}}(\Delta f) \tag{56}$$

Hypothetical ex. plot of all components? (in disco?)

3 Loop Filter Design Automation

The automation approach for ADPLL loop filter design implemented in this work will be outlined here.

3.1 Design sequence

Design automation for ADPLL loop filter is implemented with a strategy that is illustrated in figure 14, that utilizes a continuous time-approximation based model of the PLL to generate a loop filter design which minimizes the total integrated phase noise power out of the PLL. The optimized continuous filter then undergoes discrete time conversion and mapping into digital representation of the design. Second order optimization is then applied to the discretized and digitized filter implementation, to minimize effects of quantization error and filter design error due to finite word effects. A discrete-time, behavioral PLL simulator is then used to verify the filter design for proper lock-time, phase noise and stability. The following sections will detail these processes.

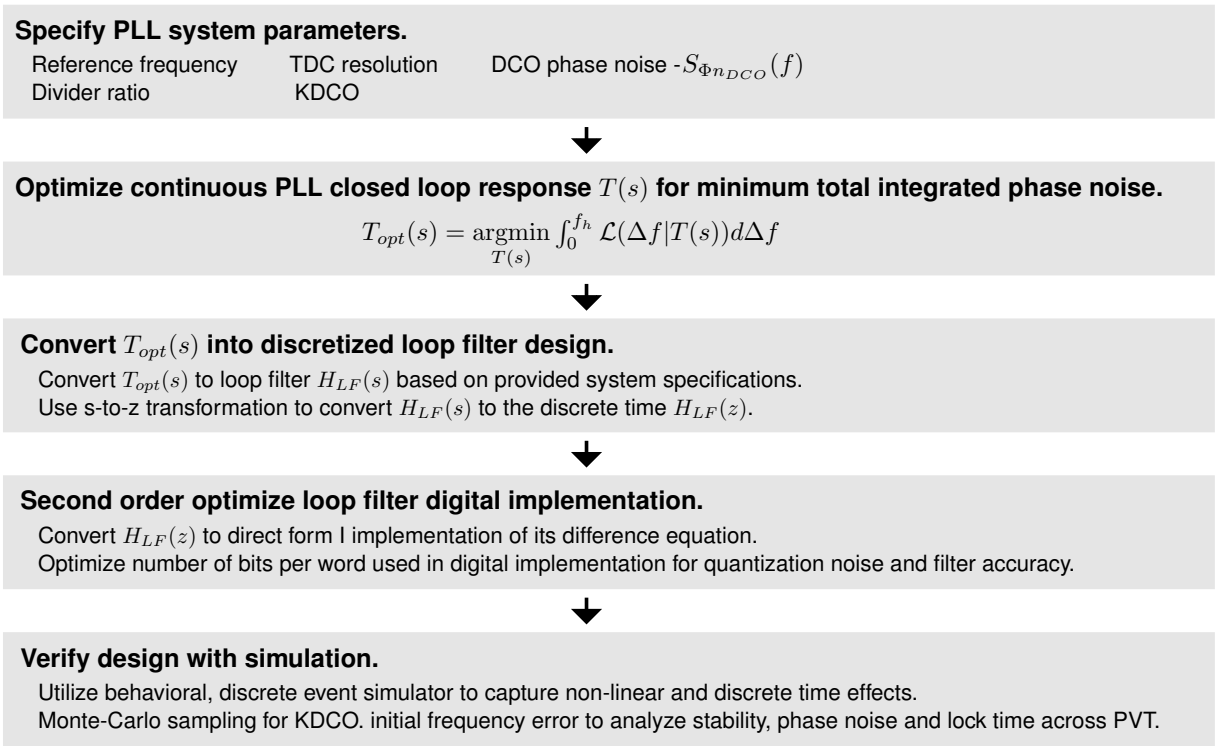

Figure 14: Filter design sequence.

3.2 Loop filter Prototype

The design automation approach developed utilizes a fixed loop filter as a prototype for all loop filter designs. This choice was derived from several criteria that were establish for desirable ADPLL operation:

1. Zero steady state phase error, to ensure accuracy of synthesized frequency.
2. Loop filter output should remain constant if input (phase error) goes to 0.
3. Minimize complexity of implemented logic, i.e. minimize number of poles and zeros.
4. Low pass response of PLL in closed-loop.

To satisfy criterion 1, the loop filter response must include an integrator (1/s) term in the transfer function [7]. A PLL with loop filter containing such an integrator is commonly classified as type II, and sans the integrator is type I [4]. A rational starting point is to consider a proportional-integral-derivative (PID) controller [8] for the loop filter, whose transfer function is given in equation 57. This filter contains coefficients K_d, K_p, K_i which set the gain of the derivative (s), proportional and integral (1/s) terms respectively.

$$\mathrm{H}_{LF}(s) = sK_d + K_p + \frac{K_i}{s} = \frac{K_d}{s}\left(s^2 + s\frac{K_p}{K_d} + \frac{K_i}{K_d}\right) \tag{57}$$

Application of the loop filter to the continuous PLL transfer function model from section 2.1.6 produces the PLL loop gain in 58 and the closed PLL loop response in 59.

$$\mathrm{L}(s) = \mathrm{H}_{LF}(s)\mathrm{H}_{VCO}(s)\mathrm{H}_{div}(s) = \frac{2\pi K_{VCO}K_d}{\mathrm{N}}\frac{1}{s^2}\left(s^2 + s\frac{K_p}{K_d} + \frac{K_i}{K_d}\right) \tag{58}$$

$$\mathrm{T}(s) = \frac{\Phi_{out}(s)}{\Phi_{ref}(s)} = \frac{2\pi K_{VCO}\left(s^2K_d + sK_p + K_i\right)}{s^2\left(1 + \frac{2\pi K_{VCO}K_d}{\mathrm{N}}\right) + \frac{2\pi K_{VCO}}{\mathrm{N}}\left(sK_p + K_i\right)} = \mathrm{N}\frac{\mathrm{L}(s)}{1 + \mathrm{L}(s)} \tag{59}$$

It should be noted that in the closed loop configuration, this PLL phase transfer function contains two poles and two zeros. This is not a low pass response as desired per criterion 4, needed for satisfactory PLL phase noise power spectrum as will later be discussed. In order achieve low pass operation, the derivative term K_d must be set to zero, yielding a proportional-integral (PI) controller for the loop filter:

$$\mathrm{T}(s) = \frac{\Phi_{out}(s)}{\Phi_{ref}(s)} = \frac{2\pi K_{VCO}\left(sK_p + K_i\right)}{s^2 + \frac{2\pi K_{VCO}}{\mathrm{N}}\left(sK_p + K_i\right)} = \mathrm{N}\frac{\mathrm{L}(s)}{1 + \mathrm{L}(s)} \tag{60}$$

Steady state zero phase error can be verified by solving the closed loop $\Phi_e(s)$ for s=0:

$$\Phi_e(s)|_{s=0} = \left(\Phi_{ref}(0) - \frac{\Phi_{out}(0)}{\mathrm{N}}\right) = \Phi_{ref}(0)\left(1 - \frac{\Phi_{out}(0)}{\mathrm{N}\Phi_{ref}(0)}\right) = \Phi_{ref}(0)\left(1 - \frac{\mathrm{N}}{\mathrm{N}}\right) = 0 \tag{61}$$

3.2.1 Continuous PI-loop filter design

Given a PI-controller loop filter, which can be optionally represented using a pole at zero and a zero with $\omega_z = K_i/K_p$:

$$\mathrm{H}_{LF}(s) = K_p + \frac{K_i}{s} = \frac{K_i}{s}\left(\frac{s}{\omega_z} + 1\right) \tag{62}$$

Selection of (not-necessarily optimal) PI controller gains can be easily derived from overall PLL settling time requirements. Suppose that settling time t_s is defined such that the PLL settles within $\pm\delta$ of the final value for a step input. If the initial and final PLL output frequencies are f_i and Nf_{ref}, and settling with $\pm f_{tol}$ is desired, $\delta = f_{tol}/|f_i - Nf_{ref}|$. Setting time is therefore:

$$t_s = -\tau \ln(\delta) \tag{63}$$

Thus, to find settling time, a value for the PLL time constant τ must be derived. Rewriting equation 60 with substitutions $\omega_z = K_i/K_p$ and $\mathrm{K} = 2\pi K_{VCO}K_i/\mathrm{N}$:

$$\frac{\Phi_{out}(s)}{\Phi_{ref}(s)} = \mathrm{N} \cdot \frac{s\frac{K}{\omega_z} + K}{s^2 + s\frac{K}{\omega_z} + K} \tag{64}$$

If the second order denominator can be redefined in terms of a natural frequency ω_n and damping ζ, such that:

$$s^2 + s\frac{K}{\omega_z} + K = s^2 + s2\zeta\omega_n + \omega_n^2 \tag{65}$$

It is then found that $\omega_n = \sqrt{K}$, and $\omega_z = \sqrt{K}/2\zeta$. The poles of equation 64 are then located at s = $\zeta\sqrt{K} \pm \sqrt{K}\sqrt{1-\zeta^2}$. The settling time of the PLL will be determined by the real portion of dominant pole of equation 64, specifically $\tau = 1/|\min(\Re(\{s_{p1}, s_{p2}\}))|$. Based on the pole-zero plot of figure 15, it can be observed that the dominant pole location is maximized with $\zeta = 1$. The pole-zero loci orientations are based on increasing ζ values. According to Razavi [13], ζ is usually "chosen to be $> \sqrt{2}/2$ or even 1 to avoid excessive ringing."

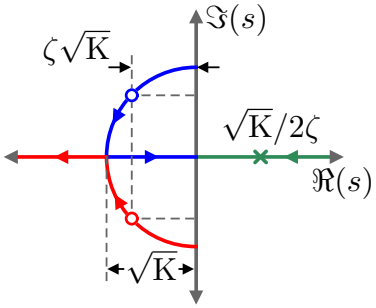

Figure 15: PI-controller PLL pole-zero locations.

To illustrate the effect of the damping coefficient ζ, figure 16 illustrates the example frequency and step responses of a PI-controlled PLL with N=1. Notice excessive peaking and ringing for $\zeta < \sqrt{2}/2$. The peaking observed in the frequency response is unavoidable with the PI-PLL due to the inherent zero in the transfer function. Its effect can be reduced with large ζ, however this will increase PLL settling time.

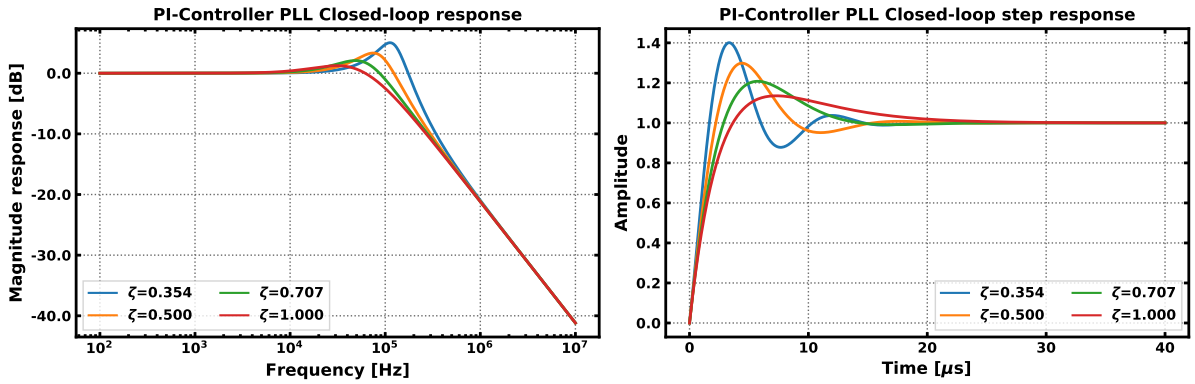

Figure 16: Example PI-PLL responses with varied ζ.

If ζ is constrained to ≤ 1:

$$\tau = \frac{1}{|\min(\Re(\{s_{p1}, s_{p2}\}))|} = \frac{1}{\zeta\sqrt{K}} \tag{66}$$

Thus:

$$t_s = \frac{-\ln(\delta)}{\zeta\sqrt{K}} = \frac{-\ln\left(\frac{f_{tol}}{|f_i - N f_{ref}|}\right)}{\zeta\sqrt{K}} \tag{67}$$

Based on specification for settling time and damping ζ, the values for K and ω_z can be determined. If K_{VCO} and N are also specified, the PI gain coefficients can be solved

additionally.

$$\omega_z = \frac{-\ln(\delta)}{2t_s} = \frac{-\ln\left(\frac{f_{tol}}{|f_i - N f_{ref}|}\right)}{2t_s} \tag{68}$$

$$K = \frac{\ln^2(\delta)}{\zeta^2 t_s^2} = \frac{\ln^2\left(\frac{f_{tol}}{|f_i - N f_{ref}|}\right)}{\zeta^2 t_s^2} \tag{69}$$

$$K_i = \frac{\mathrm{NK}}{2\pi K_{VCO}} \tag{70}$$

$$K_p = \frac{K_i}{\omega_z} \tag{71}$$

3.2.2 PI-controller peaking compensation

To compensate for closed loop peaking, the original PI-controller loop filter of equation 62 can be modified with the addition of a single tunable pole at ω_p. The closed loop response becomes third order, which complicates direct analysis and design of the loop filter, but can be handled utilizing the numerical optimization approach described in this work.

$$\mathrm{H}_{LF}(s) = \frac{K_i}{s} \frac{\left(\frac{s}{\omega_z} + 1\right)}{\left(\frac{s}{\omega_p} + 1\right)} \tag{72}$$

3.2.3 Alternative PID controller permutations

If individual terms within the PID-controller are dropped, different controller permutations (PD, ID, PI, P, I, D) can be achieved. As mentioned before, inclusion of an integral term is needed to ensure the desired zero steady state error for a PLL, and the derivative term must be removed to achieve low pass response in the PLL. This leaves integral term only controller as the remaining cantidate for PID controller design. Thus, setting the K_p and K_d terms of equation 59 to zero yields:

$$\frac{\Phi_{out}(s)}{\Phi_{ref}(s)} = \frac{2\pi K_{VCO} K_i}{s^2 + \frac{2\pi K_{VCO}}{\mathrm{N}} K_i} \tag{73}$$

This closed loop transfer function results in a pair of poles at $\pm\sqrt{2\pi K_{VCO} K_i / \mathrm{N}}$. This is not stable, as it can only be manifested as (1) a pair of poles on the imaginary axis, which is an oscillator, or (2) a real pole in the right-half plane and a real pole in the left-half plane, the former of which is not causally stable. Thus a PI-controller is the only viable PID-controller permutation for use in a PLL loop filter.

3.2.4 Discretized Loop Filter Prototype

Using the continuous filter discretization approach described in section 2.2.3 on the loop filter of equation 72 results in equation 74.

$$\mathrm{H}_{LF}(z) = \frac{K_i}{s}\frac{\left(\frac{s}{\omega_z}+1\right)}{\left(\frac{s}{\omega_p}+1\right)}\Bigg|_{s=\frac{1}{\Delta T_s}(1-z^{-1})} = k_i \Delta T_s \frac{\omega_p}{\omega_z}\frac{(1+\omega_z\Delta T_s)-z^{-1}}{(1+\omega_p\Delta T_s)-z^{-1}(2+\omega_p\Delta T_s)+z^{-2}} \tag{74}$$

The transformation of 74 into a digitally implementable design as a direct form 1 IIR filter shown in figure 17. Its filter coefficients given by equations 75-76.

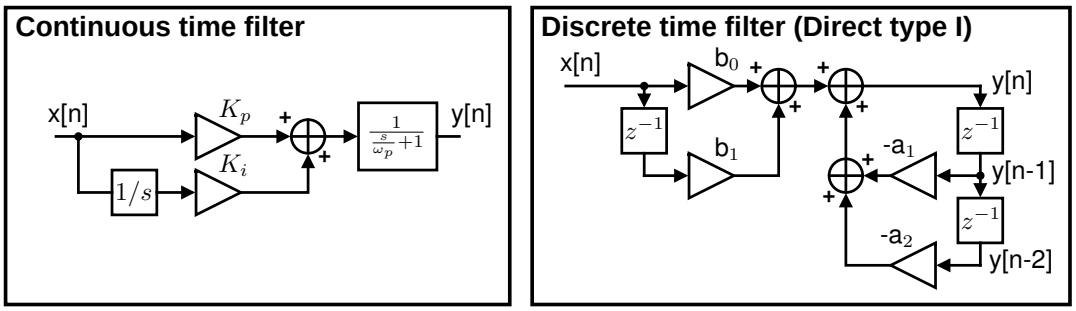

Figure 17: Implementation of filter.

$$a_1 = -\frac{2+\omega_p\Delta T_s}{1+\omega_p\Delta T_s} \qquad a_2 = \frac{1}{1+\omega_p\Delta T_s} \tag{75}$$

$$b_0 = \frac{K_i\omega_p\Delta T_s}{\omega_z}\frac{1+\omega_z\Delta T_s}{1+\omega_p\Delta T_s} \qquad b_1 = \frac{K_i\omega_p\Delta T_s}{\omega_z}\frac{1}{1+\omega_p\Delta T_s} \tag{76}$$

3.2.5 Prototype PLL response

Based on the prototype loop filter developed, the PLL closed loop response is developed for usage in the loop optimizer discussed in this work. Applying the discrete-time PLL transfer function model developed in section 2.2.5, the PLL loop gain is in equation 78, and the closed loop transfer function of the PLL is in 79.

$$\mathrm{L}(z) = \mathrm{H}_{TDC}(z)\mathrm{H}_{LF}(z)\mathrm{H}_{DCO}(z)\mathrm{H}_{DIV}(z) \tag{77}$$

$$= 2\pi K_{DCO}K_i\Delta T_s^2\frac{\mathrm{M}}{\mathrm{N}}\frac{\omega_p}{\omega_z}\frac{(1+\omega_z\Delta T_s)-z^{-1}}{(1+\omega_p\Delta T_s)-z^{-1}(3+2\omega_p\Delta T_s)+z^{-2}(3+\omega_p\Delta T_s)-z^{-3}} \tag{78}$$

The closed loop z-domain PLL phase transfer function is:

$$\mathrm{T}(z) = \frac{\Phi_{out}(z)}{\Phi_{ref}(z)} = \frac{2\pi K_{DCO} K_i \Delta T_s^2 \mathrm{M} \frac{\omega_p}{\omega_z}(1 + \omega_z \Delta T_s) - z^{-1}}{\left((1 + \omega_p \Delta T_s + 2\pi K_{DCO} K_i \Delta T_s^2 \frac{\mathrm{M}}{\mathrm{N}} \frac{\omega_p}{\omega_z}(1 + \omega_z \Delta T_s)) - z^{-1}(3 + \right.} \\ \left. 2\omega_p \Delta T_s + 2\pi K_{DCO} K_i \Delta T_s^2 \frac{\mathrm{M}}{\mathrm{N}} \frac{\omega_p}{\omega_z}) + z^{-2}(3 + \omega_p \Delta T_s) - z^{-3} \right) \tag{79}$$

Applying z-to-s domain transformation, the continuous s-domain approximation of the loop gain is given in equation 80, and the closed loop transfer function in equation 81.

$$\mathrm{L}(s) = \mathrm{H}_{TDC}(s)\mathrm{H}_{LF}(s)\mathrm{H}_{DCO}(s)\mathrm{H}_{DIV}(s) = \frac{\mathrm{M}}{\mathrm{N}} \frac{K_{DCO} K_i}{s^2} \frac{\left(\frac{s}{\omega_z} + 1\right)}{\left(\frac{s}{\omega_p} + 1\right)} \tag{80}$$

$$\mathrm{T}(s) = \frac{\Phi_{out}(s)}{\Phi_{ref}(s)} = \frac{\mathrm{M} K_{DCO} K_i \left(\frac{s}{\omega_z} + 1\right)}{s^3 \frac{1}{\omega_z} + s^2 + \frac{\mathrm{M}}{\mathrm{N}} K_{DCO} K_i \left(\frac{s}{\omega_z} + 1\right)} = \mathrm{N} \frac{\mathrm{L}(s)}{1 + \mathrm{L}(s)} \tag{81}$$

4 Behavioral ADPLL simulation

To fully capture the effects of a discrete time PLL with digital quantization effects, the implementation a behavioral, discrete event PLL simulator is described in the following. The simulator utilizes behavioral models to describe the individual components which comprise the PLL. These components are (1) a clock reference, (2) a TDC, (3) a loop filter, (4) a DCO, and (5) a divider. These behavioral models fully encapsulate effects of time-quantization and digitization. The simulator operates by iterating in fixed time steps of Δt=1/fs, where each node in the PLL is updated based upon the previous node values in a manner that is defined by each PLL component behavioral model. Each behavioral model is represented programmatically utilizing classes. In simulation, each component instance is represented by a object instance of the respective model class, constructed with any initial parameters (such as division ratio) that describe the component.

4.1 Simulation engine

The simulator engine for this work follows the sequence illustrated in figure 18 for running a simulation. Given specifications for simulation conditions (listed in the figure), the simulator accordingly initializes model objects that constitute the PLL components in simulation space. Then the simulation is run by entering a simulation loop.

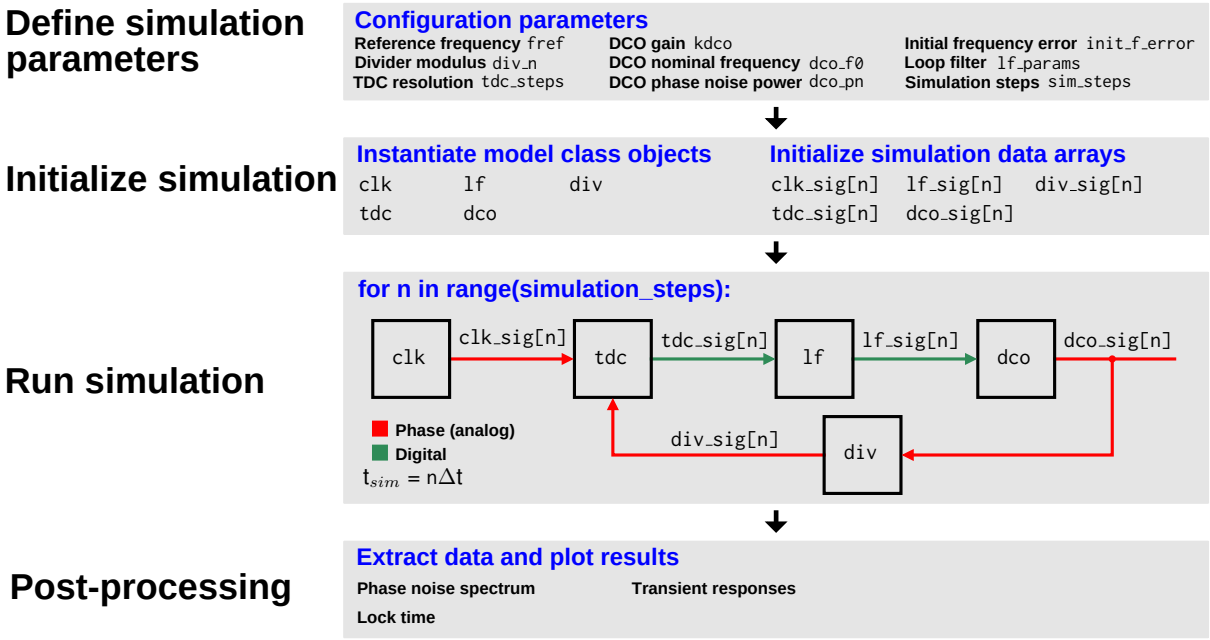

Figure 18: Simulation process.

The discrete event simulator loop is given in the following pseudocode of listing 1, with component model objects {clk, tdc, lf, dco, div}, and simulation data arrays {clk_sig, tdc_sig, lf_sig, dco_sig, div_sig}. The simulation operates with a fixed, discrete time step. Each model object is updated at each simulation step (loop iteration) utilizing the class method update, passing any relevant simulation data as arguments to the method. The output state of each component is saved into the respective array instance for each simulation step.

```
for n in range(simulation_steps):
    clk_sig[n] = clk.update()
    tdc_sig[n] = tdc.update(clk_sig[n-1], div_sig[n-1]))
    lf_sig[n]  = lf.update(tdc_sig[n-1], clk_sig[n-1]) #loop filter
    osc_sig[n] = dco.update(lf_sig[n-1])
    div_sig[n] = div.update(osc_sig[n-1], div_n)
```

Listing 1: PLL simulation loop Python pseudocode

After the simulation loop reaches completion, the results stored in the simulation data arrays can be post-processed to extract phase noise data, transient behavior and lock time. The following sections will discuss in more detail the implemented behavioral model classes and post-processing.

4.2 Clock behavioral model

An ideal behavioral clock model is utilized, given in the pseudocode of listing 2. The model is instantiated with the clock frequency f and the simulator time step dt. The model incrementing its phase every simulation step by a fixed amount $\Delta\Phi = 2\pi \mathtt{f} \cdot \mathtt{dt}$, as in 86. The model outputs an analog phase signal.

$$\Phi_{clk}[n] = \Phi_{clk}[n-1] + 2\pi \mathtt{f} \cdot \mathtt{dt} \tag{82}$$

```
class Clock:
  def __init__(self, f, dt):
    self.f = f      # clock frequency
    self.dt = dt    # simulation time step
    self.phase = 0.0  # clock phase state variable

  def update(self):
    self.phase += 2*pi*self.f*self.dt   # increment phase
    return self.phase
```

Listing 2: Ideal clock behavioral model.

4.3 TDC behavioral model

The TDC behavioral model takes two analog inputs x and y that are in units of phase, and outputs a digital word that quantifies the phase separation of the signals. The model is instantiated with a resolution parameter tdc_steps, which defines the number of phase steps per cycle of the reference input x the TDC can resolve. The method round quantizes an floating point argument to the nearest integer.

$$\text{out}[n] = \left\lfloor 0.5 + \texttt{tdc\_steps}\frac{\text{x}[n] - \text{y}[n]}{2\pi} \right\rfloor \tag{83}$$

```
class TDC:
  def __init__(self, tdc_steps):
    self.tdc_steps = tdc_steps

  def update(x, y):
    ph_error = wrap(x-y)  # wraps phase to be within [0, 2*pi]
    return round(self.tdc_steps*(ph_error/(2*pi)))
```

Listing 3: TDC behavioral model.

4.4 Loop filter behavioral model

The loop filter model implements a discrete-time filter via difference equation that operates on input x. The equivalent of one pole and two zeros are modelled, described using the filter coefficients $\{a_1, a_2; b_0, b_1\}$:

$$\text{H}_{LF}(z) = \frac{b_0 + b_1 z^{-1}}{a_0 + a_1 z^{-1} + a_2 z^{-2}} \tag{84}$$

$$\text{y}[n] = -a_1\text{y}[n-1] - a_2\text{y}[n-2] + b_0\text{x}[n] + b_1\text{x}[n-1] \tag{85}$$

Pseudocode for implementation of the model class is as follows. Data is to be represented with fixed point format, with number of fractional bits frac_bits and number of integer bits int_bits. The method fixed_point rounds floating point values to be equivalent to the nearest representation in the desired fixed point format. The filter coefficients are assumed to be pre-converted to the desired fixed-point equivalent values, and input x is assumed to be integer-valued.

```
class LoopFilter:
  def __init__(self, a1, a2, b0, b1, int_bits, frac_bits):
    self.a1 = a1; self.a2 = a2
    self.b0 = b0; self.b1 = b1
    self.xprev1 = 0;
    self.yprev1 = 0; self.yprev2 = 0
```

```
    self.int_bits=int_bits; self.frac_bits=frac_bits

  def update(x):
    ynew = -self.a1*self.yprev1 - self.a2*self.yprev2 \\
         + self.b0*x + self.b1*self.xprev1  # difference equation
    self.yprev2 = self.yprev1
    self.yprev1 = fixed_point(ynew, self.int_bits, self.frac_bits)
    self.xprev1 = x
    return round(self.yprev1) # convert to integer
```

Listing 4: Loop filter behavioral model.

4.5 DCO behavioral model

The DCO is modeled similar to the clock model, with the inclusion of a digital input `otw` for tuning the frequency. Nominal oscillator frequency is given by `f0`, and the DCO gain in Hz/LSB of `otw` is `kdco`. Additionally, modeling of the $\propto f^-2$ oscillator phase noise component, which is equivalent to random phase walk [15], is included utilizing additive random phase walk. Random walk is implemented by stochastically either adding or subtracting a fixed magnitude random walk phase increment `krw` to the oscillator phase every simulation step. The sign of `krw` is randomly chosen with equal probability for positive and negative (sampling a bi-delta distribution), implemented with the method `choice`.

$$\Phi_{osc}[n] = \Phi_{osc}[n-1] + 2\pi(\texttt{f0} + \texttt{otw} \cdot \texttt{kdco}) \cdot \texttt{dt} \pm \texttt{krw} \tag{86}$$

```
class DCO:
  def __init__(self, f0, kdco, krw, dt):
    self.f0 = f0    # nominal frequency
    self.kdco = kdco  # DCO gain
    self.krw      # random phase walk gain
    self.dt       # simulation time step size
    self.phase = 0    # phase state variable

  def update(otw):
    self.phase += 2*pi*(self.f0 + otw*self.kdco)*self.dt + krw*choice
       ([-1,1])
    return self.phase
```

Listing 5: DCO behavioral model.

Selection of the parameter `krw` to achieve a target phase noise level $\mathcal{L}(\Delta f)$ at offset Δf from the carrier is as follows.

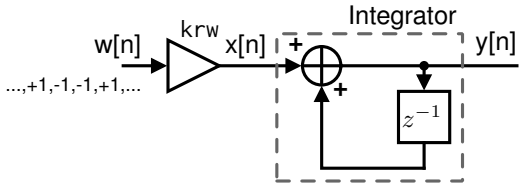

Figure 19: Discrete model for oscillator random walk.

The random walk process described in the behavioral model is represented in figure 19, where a random white-spectrum input sequence w[n] taking on values $\pm$ 1 with equal probability are multiplied by gain krw, yielding signal x[n] that is passed a discrete integrator. The output y[n] is then the phase noise signal that is summed with the oscillator phase trajectory. If the simulation is limited to sim_steps samples, Parseval's theorem for the discrete Fourier transform (DFT) in 87 results in the estimate of the power of x[n] (σ_x^2) in 88.

$$\sum_{n=0}^{\texttt{sim\_steps}-1} |\texttt{krw} \cdot w[n]|^2 = \sum_{k=0}^{\texttt{sim\_steps}-1} |X[k]|^2 \tag{87}$$

$$\sigma_x^2 = |X[k]|^2 = \texttt{krw}^2 \tag{88}$$

Computation of the spectrum of the output $y[n]$ of figure 19 can be computed as follows, recalling that $x[n]$ is white with power σ_x^2, and approximating $z = 1 - s\texttt{dt}$ is in 89. Normalizing by the number of samples sim_steps to compute spectral density is performed in 90

$$|Y(f)|^2 = |X(z)|^2 \frac{1}{|1 - z^{-1}|^2}\bigg|_{z^{-1}=(1-j2\pi f\texttt{dt})} = \frac{\sigma_x^2}{|j2\pi f\texttt{dt}|^2} = \frac{\texttt{krw}^2}{(2\pi f\texttt{dt})^2} \tag{89}$$

$$|\hat{Y}(f)|^2 = \frac{\texttt{krw}^2}{\texttt{sim\_steps} \cdot (2\pi f\texttt{dt})^2} \tag{90}$$

Given the target phase noise level $\mathcal{L}(\Delta f)$ at offset Δf, we set $f = \Delta f$ and $|Y(\Delta f)|^2$=$\mathcal{L}(\Delta f)$, a reorganization of 89 results in equation 91.

$$\texttt{krw} = 2\pi\Delta f \cdot \texttt{dt}\sqrt{\mathcal{L}(\Delta f) \cdot \texttt{sim\_steps}} \tag{91}$$

plot of phase noise from model.

4.6 Divider behavioral model

The divider model is definied with the divider modulus div_n and only performs a simple division of input phase.

```
1 class Divider:
2   def update(x, div_n):
```

```
3     return x/div_n
```

Listing 6: Divider behavioral model.

4.7 Post processing: lock time detection

Lock time detection of the PLL start-up transient can be determined from the simulation data conditioned on a tolerance band for acceptable frequency error `lock_f_tol` is provided to the simulator by the user. Since the desired frequency of the PLL `fosc = div_n*fref`, nominal oscillator frequency `dco_f0` and simulation conditions of the PLL are known by the simulator, the ideal value of the loop filter at lock, `lf_lock_ideal` can be computed directly. Given the DCO gain value in the simulation `kdco`, the value of `lf_lock_ideal = round((fosc - dco_f0)/kdco)`. Lock is then detected at the first simulation step for which the current and all later time steps meet the following criteria for the loop filter signal `lf_sig` (i.e. frequency of oscillator is within the frequency tolerance band):

$$\texttt{abs(lf\_sig[n] - lf\_lock\_ideal)*kdco < lock\_f\_tol} \tag{92}$$

This measurement is predicated on the simulation being fully complete at the time of measurement. Lock time is computed by multiplying the simulation index of lock with the simulation time step, 1/`fs`.

4.8 Post processing: phase noise power spectrum estimate

The simulation data can be used to make an estimate of the single side band phase noise power spectrum $\mathcal{L}(\Delta f)$ of the PLL (normalized to the carrier power). First, the phase error signal of the simulated PLL must be computed, `phase_error = div_n*clk_sig - osc_sig`. The phase error signal includes the phase noise signal in addition to any transient phase error components of the PLL. If the simulated PLL is in lock, the phase error can be is dominated by phase noise components, as the transient components become negligible. If `phase_error` is reduced to the simulation signal span after the detection of lock, with a span in samples of `n_steps`, the power spectral density of the phase noise normalized to the carrier tone, utilizing the fast Fourier transform (FFT) is:

$$\texttt{psd} = \left| \frac{1}{\texttt{n\_steps}} \cdot \mathcal{FFT}\{\texttt{div\_n*clk\_sig - osc\_sig}\} \right|^2 \tag{93}$$

Provided the simulation sampling rate `fs`, the indices [0, `n_steps`/2-1] of the FFT and consequently `psd` correspond to frequencies [0, `fbin`·(`n_steps`/2-1)], where `fbin` = `fs`/`n_steps`. Slicing the power spectrum data `psd` with indices [1, `fbin`·(`n_steps`/2-1)] will yield the single side band spectrum of the oscillator, with the corresponding offset frequency

of each index k being Δfk*fbin. Thus:

$$\mathcal{L}(\Delta f) = \texttt{psd[round(}\Delta f\texttt{/fbin)]} \tag{94}$$

AR model for fitting of phase noise. PSD using FFT has high variance, so use autoregressive model of order p, AR(p), fitted using Yule-Walker equations to perform better estimate of phase noise.

4.9 Monte-Carlo sampling

The simulation code implemented uses a Python dictionary containing the simulation parameters and the corresponsing parameters for which the simulation engine should simulate the PLL for. This format makes the introduction of Monte-Carlo sampling into the simulator straightforward. This can be implementing utilizing a dictionary with the nominal simulation configuration, and then a second dictionary to define the parameters to be varied along with the corresponding parameter variance. Given a sample size of N for the Monte-Carlo simulation, a loop is implemented which creates a new simulation configuration dictionary each loop iteration with stochastically sampled values from a normal distribution based on the provided nominal configuration and variance dictionaries. That unique configuration dictionary instance is used to spawn a PLL simulation, and is stored. After N iterations, N sets of data are created with varied parameters.

5 Loop filter optimization

The loop filter optimization engine implemented utilizes constrained optimization to minimize total phase noise of the PLL subject to lock time constraints. The optimizer is limited to optimizing for a loop filter in the form of 95, having parameters K_i, ω_p, ω_z. Following the theory of section 2.2, the PLL will have open loop and normalized closed loop transfer functions $\mathrm{L}(s)$ and $\hat{\mathrm{T}}(s)$ in 96 and 97 respectively. Computationally fast methods utilizing the continuous closed-loop PLL approximation $\hat{\mathrm{T}}(s)$ to estimate PLL settling time and phase noise are implemented as cost functions for the optimizer.

$$\mathrm{H}_{LF}(s) = \frac{K_i}{s}\frac{(\frac{s}{\omega_z}+1)}{(\frac{s}{\omega_p}+1)} \tag{95}$$

$$\mathrm{L}(s) = \frac{K}{s^2}\frac{(\frac{s}{\omega_z}+1)}{(\frac{s}{\omega_p}+1)} \tag{96}$$

$$\hat{\mathrm{T}}(s) = \frac{\mathrm{L}(s)}{1+\mathrm{L}(s)} = \frac{K}{s^2}\frac{(\frac{s}{\omega_z}+1)}{(\frac{s}{\omega_p}+1)} \tag{97}$$

Filter optimization follows the following sequency:

1. Minimize integrated phase noise with $\hat{\mathrm{T}}(s)$ definition of closed loop behavior. Yields optimal $\{K, \omega_p, \omega_z\}$.
2. Translate optimal parameters to prototype loop filter parameters, perform continuous to discrete time filter conversion.
3. Optimize fixed point resolution of digital loop filter implementation for finite word effects.

The following sections detail the optimizer methods implemented.

5.1 Fast estimation of PLL settling time

Based on the continuous model approximation of ADPLL dynamics, the PLL closed loop phase transfer function $\hat{\mathrm{T}}(s)$ is defined as a rational function of two polynomial functions of s, with P poles and Z zeros. Such a transfer function is computationally represented with arrays A and B, containing the denominator and numerator polynomial coefficients.

$$\hat{\mathrm{T}}(s) = \frac{\sum_{j=0}^{Z} b_j s^j}{\sum_{k=0}^{P} a_n s^n} \tag{98}$$

An estimate of the step response settling time of $\mathrm{T}(s)$ can by utilizing its representation in state space. This is given in 99, with input vector $\mathrm{U}(s)$, state vector $\mathbf{X}(s)$, and output $Y(s)$. The state-space representation from a s-domain transfer function can be quickly solved computationally with available signal processing packages such as `scipy.signal` given the coefficent arrays A and B.

$$s\mathbf{X}(s) = \mathbf{A}\mathbf{X}(s) + \mathbf{B}\mathrm{U}(s) \tag{99}$$

$$Y(s) = \mathbf{C}\mathbf{X}(s) + \mathbf{D}\mathrm{U}(s) \tag{100}$$

The set of k eigenvalues $\{\lambda_1, ..., \lambda_N\}$ corresponding to poles for the system are found as the roots of 101 [1].

$$|\mathbf{A} - \lambda\mathbf{I}| = 0 \tag{101}$$

Imposing the constraint of number of poles P $>$ number of zeros Z, the system $\mathrm{T}(s)$ may be represented via partial fraction decomposition using the poles from the eigenvalues of state matrix $\mathbf{A}$ $\{\lambda_1, ..., \lambda_N\}$:

$$T(s) = \sum_{k=1}^{P} \frac{c_k}{s - \lambda_k} \tag{102}$$

Inverse Laplace transformation shows the step response of the system will be a sum of exponentials:

$$y(t) = c_1 e^{\lambda_1 t} + ... + c_k e^{\lambda_k t} \tag{103}$$

The dynamics of the step response are governed by the exponential components of y(t). If $\{\lambda_1, ..., \lambda_N\} \in \mathbb{C}$ where $\lambda_k = 1/\tau_k + j\omega_K$, the real portion of each λ_k will describe the transient behavior of each exponential, having time constant τ_k. The long term settling of y(t) will be dominated by the exponential with the largest τ_k, i.e. the dominant pole of the system. This estimate of settling time uses the dominant pole τ_k as a heuristic estimate for overall time constant of the system, τ. Finally, settling time t_s can be considered as the time interval required for the signal to drop within a tolerance band $\pm\delta_{tol}\mathrm{y}(\infty)$ about the final value $\mathrm{y}(\infty)$. Thus:

$$t_s = \tau \ln(\delta_{tol}) = \frac{\ln(\delta_{tol})}{\min(|\Re(\{\lambda_1, ..., \lambda_k\})|)} \tag{104}$$

This settling time estimate is computationally fast, as it requires only (a) computation of state matrix $\mathbf{A}$, (b) computation of the eigenvalues of $\mathbf{A}$, and (c) computation of settling time from the eigenvalue with minimum real component.

5.2 Estimation of PLL phase noise

It is assumed here that [move discussion of this here...] the dominant output-referred phase

noise contributions of the PLL are due to the DCO thermal noise and TDC quantization. If S_{TDC} and S_{DCO} are the PLL output-referred noise PSD respectively for the TDC and DCO noise sources from section 2.3, the total PLL output noise PSD $S_\Sigma(f)$ is estimated as 105. N is the PLL divider modulus.

$$S_\Sigma(f) = S_{\Phi n_{TDC,out}}(f) + S_{\Phi n_{DCO,out}}(f) \tag{105}$$

$$= \frac{1}{12 f_{ref}} \left| 2\pi \frac{\mathrm{N}}{\mathrm{M}} \hat{\mathrm{T}}(f) \right|^2 + \frac{S_{0\Phi n_{DCO}}}{f^2} \left| 1 - \hat{\mathrm{T}}(f) \right|^2 \tag{106}$$

Given a bandwidth of interest Δf (i.e. baseband bandwidth for radio applications), the total integrated phase noise power is:

$$P_{\phi noise} = 2 \int_0^{\Delta f} S_\Sigma(f) df \tag{107}$$

This can be computation solved for a grid of K values in the interval Δf, where each point represents a frequency bin f_{bin} = Δf/K. Therefore this estimate is implemented as such:

$$\hat{P}_{\phi noise} = 2 \sum_{k=0}^{K-1} S_\Sigma(k f_{bin}) f_{bin} \tag{108}$$

Utilize Romberg method for numerical integration, it has high accuracy for smooth integrands - [2].

5.3 Loop filter optimization algorithm

The optimization algorithm in use is predicated on a fixed form for the filter being design, as in 95, and consequenctly known and fixed open and closed loop transfer function forms. The prototype loop filter design in this work a contains a tunable pole ω_p, a tunable zero ω_z and a gain parameter K. To allow the phase noise minimization and the constraint on maximum lock time to both have an impact in the optimization, the optimization is implemented with two nested levels. There is there is a lower level optimizer which will minimize phase noise given a fixed target for settling time. The higher level optimizer applies a constrained search for settling time, utilizing the lower level optimizer, that results in minimum phase noise.

Level A - Minimize phase noise for fixed settling time.

- Minimize phase noise while maintaining fixed settling time = t_s.
- **Solution:** use two steps per interation until satisfactorily converged:

  1. Minimize phase noise using pole/zeros locations (gradient descent).
  2. Tune K such that settling time = t_s (golden section search).

Level B - Optimize settling time given constraints.

- Use golden section search to find optimal constrained settling time that has minimal phase noise using method from level A as cost function.

5.4 Loop filter optimization - finite word effects

Once a filter design has been optimized in the continuous domain following section 5.3, second order optimization is carried out to ensure the digitized, discrete implementation performs as expected in the presence of finite word effects. The optimized digital implementation provided here utilized fixed-point words for equal resolution throughout the datapath. The implemented second order optimization considers both the effect of loop filter quantization noise and transfer function error.

Loop filter quantization noise optimization

6 Discussion and results

- Discuss choices made in simulator
- show effects of non-linearity : simulate PLL without BB-PD (far from ideal)
- Low resolution: feedback stops when within 1 LSB in phase lock, response time = t=(n/(m*df)), Use bbpd to add extra resolution.
  - Deficiencies, advantages, why they were made
  - Phase noise/lock time analysis
  - Analysis - monte-carlo variation to analyze stability/lock time
  - purpose: to validate filter design
- Filter structure choice - PI with added pole. Why is this best (low complexity, no phase error)
- Why only phase random walk in oscillator phase noise
- Why direct type I implementation
- Discuss choices made in loop filter designer/optimizer
  - Why only optimize for TDC/DCO phase noise initially - (other noise sources are easier to reduce below the limits of these two). Flicker noise ignore due to time resolution limitations, expectation that reference flicker¿ PLL flicker components as reference flicker with be multiplied by N at output.
  - Plot showing BW vs noise components, motivates optimization approach. PN min when TDC and DCO components roughly equal.
  - Discuss why ref flicker noise doesn't matter (it can't be altered by PLL so it doesn't matter for optimization)
  - Optimizer approach: minimization of phase noise constrained by lock time (BFGS optimizer)
  - Second order optimization of filter design for data representation precision with discrete time considerations (first order design is with approximations from continuous PLL model). Discretized LF noise via simulation with input noise

  - Recommendations for divider noise limit
  - Design verification
- State of art comparison
  - Compare to state of art/existing frameworks?
  - Existing optimization approaches: second order PLL [14]
  - What are improvements made here?
  - Perrot's pre-existing work: general purpuse simulation architecture, doesn't directly handle optimization for integer-N, especially in heavily quantized case
- Design example - compare to existing
  - Design 2.4G PLL for WuRx, show results from process
  - Repeat in CPPsim, compare results?
  - Explain advantage of this framework based on exercise
- Discuss limitations and considerations for use of framework
  - Models are not accurate for frequencies near or greater than reference frequency???
  - Sampling rate recommendations (high oversampling)
  - Minimum choice of TDC resolution, constraints for divider jitter,
  - Optimizer needs poles¿zeros

Recommendations for maximum divider jitter, loop filter resolution

6.1 Divider noise constraint

Output refered phase noise PSD of TDC:

$$S_{\Phi n_{TDC,out}} = \frac{1}{12 f_{ref}} \left| 2\pi \frac{N}{M} G(f) \right|^2 \tag{109}$$

Output refered phase noise PSD of divider:

$$S_{\Phi n_{div,out}} = f_{ref} \left| 2\pi N \sigma_{tn_{div}} G(f) \right|^2 \tag{110}$$

The output-referred phase noise for the TDC and divider have the same frequency dependence. So by setting $S_{\Phi n_{div,out}} < S_{\Phi n_{TDC,out}}$, a constraint to force PLL output divider less than TDC noise can be found:

$$\sigma_{tn_{div}} < \frac{1}{\mathrm{M} f_{ref}} = \Delta t_{step_{TDC}} \tag{111}$$

Must simply ensure that jitter of divider is much less than TDC resolution, which is a reasonable demand. Thus, it is reasonable to ignore divider noise in the phase noise optimization if divider noise can reasonably be made insignificant in the overall output phase noise.

6.2 Example exercise

Use WuRx design specs to motivate design example... put updated/better definition of specs relative to design example

Parameter	Value	Unit	Notes
Frequency	2.4-2.4835	GHz	2.4G ISM Band
Ref. frequency	16	MHz	Yields 6 channels
Power	$\leq$ 100	μW	
Residual FM	$\leq$ 107	kHz$_{RMS}$	BER $\leq$ 1e-2, f_{dev}=$\pm$250 KHz
Initial Lock Time	$\leq$ 50	μs	Upon cold start
Re-lock Time	$\leq$ 5	μs	Coming out of standby
Bandwidth	100	kHz	(nominally), tunable

Table 1: System-level specifications

Parameter	Value	Unit	Notes
DCO LSB Resolution	$\leq$ 50	kHz	Determined from quantization noise.
DCO DNL	$<$ 1	LSB	Ensures monotonicity
TDC Resolution	$\leq$ 3.8	ns	
TDC Resolution (bits)	$\geq$ 4.03	bits	

Table 2: Component-level specifications.

7 Conclusion

Extend to fractional-N. Loop filter design will be the same, difference is divider model.

References

[1] R. Brockett. “Poles, zeros, and feedback: State space interpretation”. In: *IEEE Transactions on Automatic Control* 10.2 (1965), pp. 129–135. DOI: 10.1109/tac.1965.1098118.

[2] “Chapter 15: Numerical Integration”. In: *A First Course in Numerical Methods* (2011), pp. 441–479. DOI: 10.1137/9780898719987.ch15.

[3] F. Gardner. “Charge-Pump Phase-Lock Loops”. In: *IEEE Transactions on Communications* 28.11 (Nov. 1980), pp. 1849–1858. DOI: 10.1109/tcom.1980.1094619.

[4] Floyd Martin Gardner. “Chapter Two Loop Fundamentals”. In: *Phaselock techniques*. John Wiley, 2005.

[5] T.h. Lee and A. Hajimiri. “Oscillator phase noise: a tutorial”. In: *IEEE Journal of Solid-State Circuits* 35.3 (2000), pp. 326–336. DOI: 10.1109/4.826814.

[6] D.b. Leeson. “A simple model of feedback oscillator noise spectrum”. In: *Proceedings of the IEEE* 54.2 (1966), pp. 329–330. DOI: 10.1109/proc.1966.4682.

[7] Katsuhiko Ogata. “5-7 Effects of Integral and Derivative Control Actions on System Performance”. In: *Modern control engineering*. Prentice Hall, 2010.

[8] Katsuhiko Ogata. “Chapter 8 PID Controllers and Modified PID Controllers”. In: *Modern control engineering*. Prentice Hall, 2010.

[9] M.h. Perrott, M.d. Trott, and C.g. Sodini. “A modeling approach for Sigma-Delta fractional-N frequency synthesizers allowing straightforward noise analysis”. In: *IEEE Journal of Solid-State Circuits* 37.8 (2002), pp. 1028–1038. DOI: 10.1109/jssc.2002.800925.

[10] John G. Proakis and Dimitris G. Manolakis. “7.3 Structures for IIR Systems”. In: *Digital signal processing: principles, algorithms, and applications*. Macmillan, 1993.

[11] John G. Proakis and Dimitris G. Manolakis. “8.3.3 IIR Filter Design by the Bilinear Transformation”. In: *Digital signal processing: principles, algorithms, and applications*. Macmillan, 1993.

[12] Behzad Razavi. “Design of monolithic phase-locked loops and clock recovery circuits tutorial”. In: 1996.

[13] Behzad Razavi and Behzad Razavi. “16 Phase-Locked Loops”. In: *Design of analog CMOS integrated circuits*. McGraw-Hill.

[14] A. Spalvieri. “Optimal Loop Filter of the Discrete-time PLL in the Presence of Phase Noise”. In: *11th IEEE Symposium on Computers and Communications (ISCC06)* (2006). DOI: 10.1109/iscc.2006.115.

[15] V. Vannicola and P. Varshney. “Spectral Dispersion of Modulated Signals Due to Oscillator Phase Instability: White and Random Walk Phase Model”. In: *IEEE Transactions on Communications* 31.7 (1983), pp. 886–895. DOI: 10.1109/tcom.1983.1095902.

A Oscillator phase noise due to thermal noise

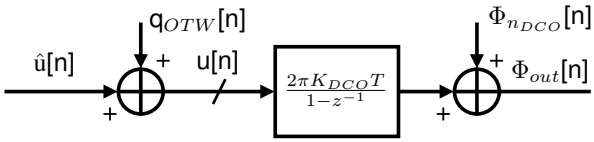

Figure 20: DCO additive noise model.

Oscillator phase noise due to stochastic and uncorrelated circuit and supply noise can be analyzed as additive voltage disturbance δv_n with variance $\sigma^2_{v_n}$ to the oscillator waveform V_{osc} at any given time. In a stable, noiseless oscillator, amplitude is inherently tied to signal phase, i.e. $V_{osc}(\Phi = \omega t)$. With additive noise, given $\frac{dV_{osc}(\Phi)}{d\Phi}$ is finite $\forall$t, a small voltage disturbance from noise δv_n will be coupled as a disturbance $\delta\Phi_n$ in the oscillator phase, shown in figure 21. The phase evolution of the noisy oscillator for an infinitesimal time increment δt with such a disturbance is:

$$\Phi_{out}(t + \delta t) = \Phi_{out}(t) + \delta\Phi_n + \omega_{osc}\delta t \tag{112}$$

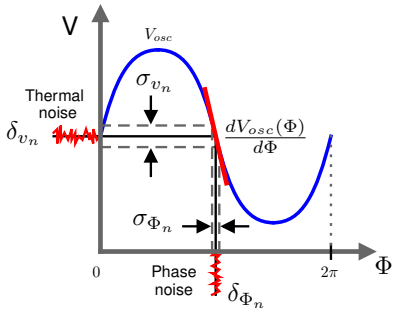

Figure 21: Voltage to phase noise conversion.

Assuming δv_n is Gaussian white noise, $\delta\Phi_n$ is sampled stochastically at any instant based on the probability distribution 113, dependent on the current oscillator phase Φ_{out} and the noiseless voltage-phase relation $V_{osc}(\Phi)$. It will be assumed that like the source noise δv_n, $\delta\Phi_n$ is white spectrum.

$$P(\delta\Phi_n|\Phi_{out}) = \text{Norm}\left(\mu = 0, \sigma = \sigma_{v_n}\left(\left.\frac{dV_{osc}(\Phi)}{d\Phi}\right|_{\Phi=\Phi_{out}}\right)^{-1}\right) \tag{113}$$

Spectral analysis of the noisy oscillator phase can be made utilizing discrete time-modeling. Converting 112 into a sampled signal with time step δt

$$\Phi_{out}[n+1] = \Phi_{out}[n] + \omega_{osc}\delta t + \delta\Phi_n[n|\Phi_{out}[n]] \tag{114}$$

Computing the z-transform, and splitting the result into the oscillation Φ_{osc} and phase noise Φ_n components:

$$\Phi_{out}(z) = \frac{\omega_{osc}\delta t}{z-1} + \frac{\delta\Phi_n(z)}{z-1} = \Phi_{osc}(z) + \Phi_n(z) \tag{115}$$

$$\Rightarrow \Phi_n(z) = \frac{\delta\Phi_n(z)}{z-1} \tag{116}$$

Application of the bilinear transform to 116 can be used to approximate the continuous phase noise spectrum, if $s = j\omega$

$$\Phi_n(s) = \Phi_n(z)|_{z=1-s\delta t} = \left.\frac{\delta\Phi_n(z)}{z-1}\right|_{z=1+s\delta t} = \frac{\delta\Phi_n(s)}{s\delta t} \tag{117}$$

The phase noise PSD is therefore:

$$S_{\Phi n_{DCO}}(f) = \lim_{\Delta T\to\infty}\frac{1}{\Delta T}\left|\frac{\delta\Phi_n(j2\pi f)}{j2\pi f\delta t} * \mathcal{F}\left\{\text{rect}\left(\frac{t}{\Delta t}\right)\right\}\right|^2 = \frac{S_{0\Phi n_{DCO}}}{f^2} \tag{118}$$

Following that the phase disturbance signal $\delta\Phi_n(t)$ is white spectrum, a constant value for its PSD $S_{0\Phi n_{DCO}}$ can be defined. The value for $S_{0\Phi n_{DCO}}$ is highly dependent on implementation and is best extracted by means of curve fitting simulation or physical measurement.